NTNU – Trondheim
Norwegian University of
Science and Technology

Power Electronics Converter for use in Direct Electrical Heating Application

Sivert Eliassen

Master of Energy and Environmental Engineering
Submission date: June 2012
Supervisor: Lars Einar Norum, ELKRAFT
Co-supervisor: Anandarup Das, ELKRAFT
Espen Haugan, Siemens AS

Norwegian University of Science and Technology
Department of Electric Power Engineering

Problem description

Direct electrical heating (DEH) is an efficient flow assurance method for subsea pipelines, which aims to prevent hydrate formation by keeping the pipeline content above a given temperature. The method is based on injecting a single phase AC current directly through the pipeline and back through a cable strapped on the top of the pipe. Traditionally, the DEH load has been supplied via a 3-phase transformer and balancing circuit directly connected to the network.

It has been suggested using a power electronics source to supply the DEH load, as this will enable desired features such as increasing flexibility in terms of power control and tuning of the system to match the load impedance. If a modular power electronics source is used, increasing power requirements can be met by stacking multiple modules to increase voltage levels.

This thesis should identify the requirements that a power electronics source must meet in order to supply a DEH load. Based on the obtained requirements, two different converter topologies, the well-known Perfect Harmony and the emerging MMC, will be evaluated with respect to suitability for this application. A basis for the thesis should be that the chosen system promotes modularity and flexibility and hence is possible to adapt to DEH systems of different sizes in an uncomplicated manner.

The most promising alternative should be studied further to address technical challenges that are identified in the process. Influence on the grid when operating a large single-phase load is believed to be among the main challenges that needs to be resolved. A simulation model of the preferred converter should be constructed, and the performance of the model and the suitability of the converter should be confirmed through simulations.

The thesis should form a basis for further studies on a power converter for DEH application.

Assignment given: 19. January 2012
Supervisor: Lars E. Norum, Department of Electrical Engineering

Preface

This report represents the end of an interesting, informative and eventful era as a master student with the Department of Electrical Engineering, NTNU. This final year has been very inspiring and has given me the opportunity to explore topics within my fields of interest, which I am very thankful for.

Many evenings have been spent in the office and working on the thesis has at times been a more of a lifestyle than a job. Luckily, I haven't been the only one writing a thesis and it is easier to keep on track when surrounded by fellow students. I would like to thank Andreas Hallan, Kenneth Tjong and Ole Christian Nebb in my office for moral support, technical advice and discussions, as well as for adding happiness and humor to the everyday work. It wouldn't have been the same without you. I would also like to thank my girlfriend for her patience and support during my final year. During late hours, she has been very understanding and encouraged me to keep going. She has also made a direct contribution by proofreading the thesis. For this I am very thankful.

My co-supervisor at Siemens, Espen Haugan, has been of great help throughout my final year as a master student. He came up with the outline of the topic for my thesis, and that way gave me the opportunity to gain knowledge in a field in which I have great interest. He has provided information, answered questions, and given me valuable feedback along the way. He has also inspired me to work those extra hours on the thesis.

A number of people at NTNU have also been of great help. Post Doc. Anandarup Das has provided help and advice, and also gave me valuable input for constructing my simulation model, saving me a lot of time. PhD-student Hamed Nademi has shared of his knowledge and assisted me in achieving desired performance of the simulation model. SINTEF researcher Harald Kulbotten has kindly shared of his detailed knowledge on DEH-systems and helped me gain an overview of the DEH concept and its related challenges.

Last but not least, I thank Professor Lars Norum, my supervisor. He has been very helpful in narrowing down the problem description, a vital contribution to keep me on track. He has also given me feedback and valuable advice throughout my final year.

Trondheim 11.06.2012
Sivert Eliassen

Abstract

Direct Electrical Heating (DEH) is a flow assurance method in subsea pipelines operating at high pressure and low temperatures and has gained ground throughout the last decade. DEH systems in operation are based on passive components operating at grid frequency. This thesis investigates the possibility of using power electronics to supply a Direct Electrical Heating (DEH) load. A power electronic converter solution will introduce increased flexibility and control, and can operate at higher frequencies, which is believed to increase overall system efficiency.

A system description treating the main components of a DEH system is given, and typical values for key parameters are presented. Requirements for a power electronic converter for DEH application are identified, and two possible converter topologies are evaluated. It is shown that both the Series-Connected H-Bridge (SC-HB) converter and the Modular Multilevel Converter (MMC) are topologies suited for DEH application, but the MMC is the only converter investigated further. Compared to the SC-HB, it offers operation within a wider voltage- and current range, a feature being important as DEH is applied to increasingly larger systems. It also offers better flexibility than the SC-HB in terms of front-end configuration, space considerations and load compensation solution.

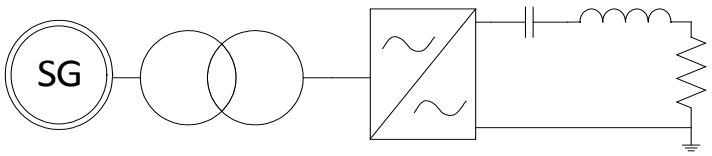

1: Outline of simulated system

A simulation model of the MMC, along with the DEH load, is constructed in MATLAB Simulink. Through detailed simulations and testing, the performance of the simulation model and control system is verified, and the model is shown to behave according to existing theory.

The pipeline being heated represents a single-phase load in the megawatt range. The instantaneous power delivered to the load will oscillate at twice the operating frequency of the converter, causing unacceptable power oscillations on the grid. To reduce these oscillations, a filter is applied on the DC-link. It is shown that a resonant band-stop LC- filter is capable of minimizing the power oscillations, and at the same time reduces internal currents and losses. The reduction of internal currents may also allow for some weight reduction, by reducing the arm inductance originally included to suppress the circulating currents.

The MMC is shown to be a suitable converter for DEH application, and it has some significant advantages compared to the existing solution based on a passive balancing circuit.

Sammendrag

Direct Electrical Heating (DEH) er en metode for å sikre strømning i gassrør som opererer under høyt trykk og lav temperatur, og har blitt tatt i bruk i flere anlegg siden årtusenskiftet. Eksisterende DEH-anlegg drives med nettfrekvens og bruker passive komponenter for å oppnå en balansert last. Denne oppgaven vurderer muligheten for å forsyne DEH-systemer via en kraftelektronikkomformer. En omformer vil gi økt kontroll og fleksibilitet, og kan også drives ved høyere frekvens. Dette antas å gi en høyere systemvirkningsgrad enn dagens løsning.

En systembeskrivelse som dekker hovedkomponentene i et DEH-system gis, og typiske verdier for sentrale parametre blir oppgitt. En kravspesifikasjon for en kraftelektronikkomformer tilpasset DEH blir utarbeidet, og to lovende topologier blir vurdert. Både Series-Connected H-bridge (SC-HB) omformer og Multilevel Modular Converter (MMC) omformer er egnet for bruk i DEH anlegg, men kun MMC omformeren har blitt evaluert i detalj. Den kan operere innenfor et større strøm- og spenningsområde sammenlignet med en SC-HB, noe som er vesentlig etterhvert som DEH blir tatt i bruk på stadig større anlegg. Den har også bedre fleksibilitet med tanke på likeretterløsning, plasseringsvennlighet og lastkomenseringsløsning.

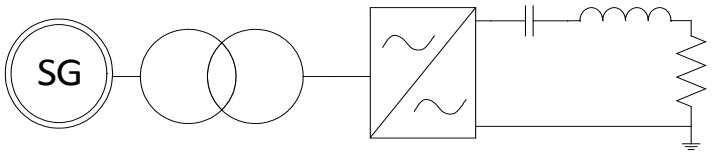

2: Skisse av simulert system

En simuleringsmodell av en MMC omformer med en DEH last har blitt bygd opp i MATLAB Simulink. Simuleringer bekrefter at modellen oppfører seg som forventet, og i tråd med eksisterende teori på området. Modellen gir grunnlag for dimensjonering av et DEH-anlegg.

Det oppvarmede røret er en enfaselast på flere megawatt. Momentaneffekten levert til lasten oscillerer med det dobbelte av utgangsfrekvensen, og gir uønsket innvirkning på nettet. Et resonant båndstopp LC-filter plassert på DC-linken minimerer effektfluktuasjoner mot nettet og holder overharmoniske strømmer innenfor grenser fastsatt av standarder. Samtidig bidrar filteret til å minimere interne strømmer i omformeren. Dette bidrar til å redusere tap, og kan også bidra til vektreduksjon ved at det muliggjør reduksjon av induktansen i armene på omformeren, som i utgangspunktet er ment å redusere de interne strømmene.

Oppgaven viser at MMC topologien er godt egnet for bruk i DEH-anlegg, og at den har flere klare fordeler sammenlignet med løsningen brukt i eksisterende anlegg.

Contents

List of figures

List of tables

Abbreviations

AC	Alternating Currrent
DC	Direct Current
DEH	Direct Electrical Heating
EMI	ElectroMagnetic Interference
FPSO	Floating Production, Storage and Offloading unit
HVDC	High Voltage Direct Current
IEEE	Institute of Electrical and Electronics Engineers
IGBT	Insulated Gate Bipolar Transistor
MMC	Modular Multilevel Converter
PCC	Point of Common Coupling
PD	Phase Disposition
PF	displacement Power Factor
PH	Perfect Harmony
PI-controller	Proportional-Integral controller
PWM	Pulse-Width Modulation
SC-HB	Series Connected H-Bridge
SM	SubModule
THD	Total Harmonic Distortion

1 Introduction

1.1 Motivation

A well-known problem related to subsea pipelines is the formation of hydrates or wax. In fact, the problem was described as early as the mid-1930's [1]. Since transport of untreated petroleum products of long distances avoids the need for costly separation facilities offshore, multiphase pipelines are very common [2]. Hydrates may form both in two-phase flow (gas-liquid, liquid-liquid), or three phase flow (gas-liquid-liquid) systems [3]. If hydrates form, they will reduce the rate of flow through the pipeline or ultimately clog the pipeline completely [3]. The formation of hydrates is dependent on the water content in the pipeline flow and occurs at low temperatures (up to 25˚C) and elevated pressure [1],[4]. These conditions are common in subsea gas transportation systems, and exploration and operation in increasingly deeper water will increase the pressure further [3]. With respect to flow assurance, this makes hydrates an important issue that must be addressed to ensure satisfactory pipeline performance. Although hydrate formation also may occur during normal operation, it is particularly a problem during shutdown conditions, where the temperature inside the pipeline will approach ambient temperature, thus making the gas/water enter the hydrate formation region [3]. This may lead to a complete blockage of the pipeline.

There are four methods for preventing formation of hydrates [1]:

1. Remove or reduce water content
2. Decrease the pressure
3. Injecting a chemical component, such as an alcohol, glycol or salt to attract water molecules
4. Increase the temperature.

All these strategies involve altering one of the three required elements for hydrate formation; pressure, water or temperature [5]. Traditionally, chemical treatment has been the preferred choice of method for hydrate prevention, but the method is expensive, and alternative solutions have emerged, focusing on heating of the pipeline [6].

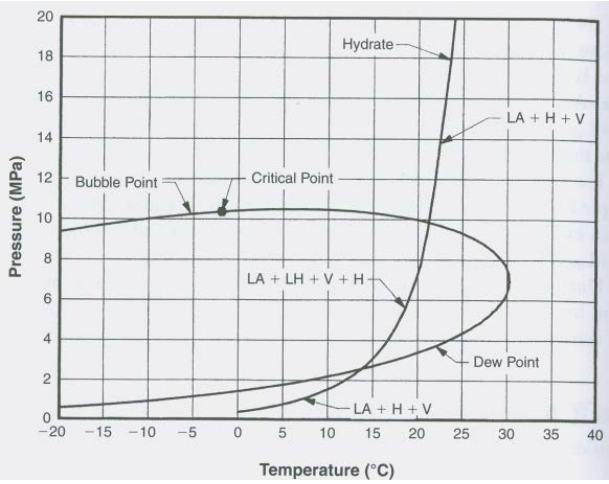

Figure 1: Phase diagram for a typical natural gas, with hydrate line indicated [7]

Figure 1 shows a typical pressure-temperature relation for the formation of hydrates. The aim of heating the pipeline is to keep the pipeline contents at a temperature where hydrates cannot form, corresponding to the area to the right of the hydrate curve in Figure 1. As the figure shows, this temperature will be pressure dependent, with higher temperatures required at greater depths.

There are different strategies in use to overcome this problem. Traditionally, an injection of chemicals (methanol) to reduce the critical temperature at which hydrates form has been the preferred solution [4] . This method is efficient with respect to avoiding hydration formation, but has large investment and operation costs. Also, as the petroleum industry moves into deeper waters, the amount of chemical inhibitors required increases, making the solution less attractive.

An alternative method that has gained ground over the past decade, is Direct Electric Heating (DEH). It is a method that, unlike the chemical approach, does not aim to lower the temperature at which hydrates are forming. Instead, it aims to keep the temperature above the critical limit, as dictated by the gas mixture and operating conditions. Heating is achieved by applying an electric current through the pipeline itself, thereby generating losses in the pipeline and keeping the gas above a given temperature, typically in the range of 25-30°C.

For the remainder of this thesis, the phenomenon of hydrates and wax in pipelines is not discussed further. It is merely accepted that it is a challenge that needs to be resolved for satisfactory pipeline performance, and that this can be achieved by maintaining the temperature inside the pipeline above a certain level. This again dictates a requirement for power dissipation from the applied electric current.

1.2 Relation to specialization project

The author wrote a report called "Efficiency improvements in Direct Electrical Heating systems by increasing operating frequency" in connection with the specialization project in the fall of 2011. Parts of this report has been used in the master thesis in order to form a more complete and independent text. This includes the following sections:

- Section 1.1: Motivation
- Section 2: General system description of the state of the art solution

In addition to this, some of the results obtained in the specialization project are used for modeling of the load. This is described in Appendix B.

2 General system description of the state of the art solution

The basic principle of Direct Electrical Heating is very simple. Heat is generated by passing AC current at grid frequency through the gas pipeline. The pipeline is grounded at both ends and along the line to avoid large voltages in the system. The amount of current to flow must be set to match the heating requirements of the pipeline. As the pipeline works as a single conductor, the current supplied must be single phase. Power is supplied from topside, either onshore or from a platform, via riser cables to the subsea pipeline system.

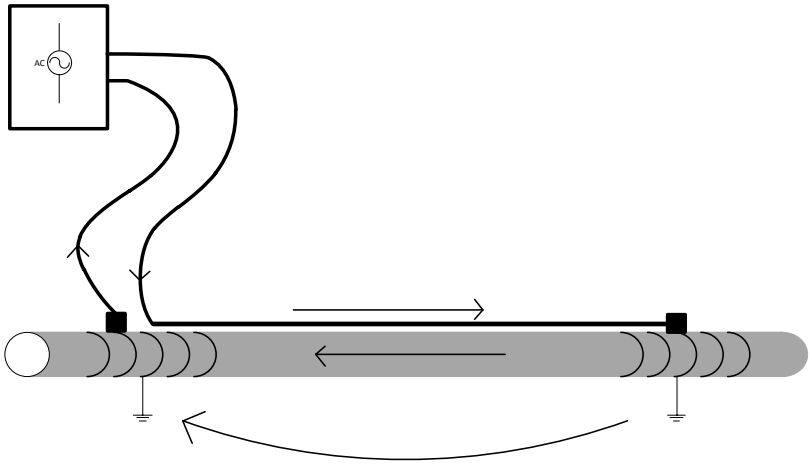

Figure 2: Basic overview of heating principle and current flow

2.1 Power requirements

The amount of active power required for a system may vary, but systems already in operation in the North Sea are in the range of 1-10 MW [8]. It is expected that DEH will be applied to systems of increasing size in the coming years, and this will lead to increasing power ratings. DEH has been installed on pipelines as long as 44km [9]. For 8"-12" pipes, a power requirement of 100-150W/m has proven to be a decent estimation for preliminary calculations [8]. In addition to the active power requirements, the pipeline system is highly inductive, and therefore consumes large amounts of reactive power, with a power factor of typically 0.25-0.30 [8], [10]. This calls for a large compensation unit onshore to produce this reactive power to avoid drawing vast amounts of reactive power from the supply network.

The required power will not only depend on the physical dimensions of the system, but also on the mode in which it is operated. The DEH system can be applied to maintain a temperature above the critical temperature at which hydrate formation occurs during normal production and pipeline flow. It can also be used to heat the system from ambient temperature after shutdowns, or for wax melting or removal of hydrate plugs etc. If the system is used to heat the pipeline after a shutdown, this will require more power than maintaining a steady temperature. For a heating

time of 48h, the power requirement might be 3 times higher than when maintaining a steady-state temperature, and this will further increase if the heating time is to be reduced [8].

Controlling the power to the described DEH system is not straight forward. The load impedance is given, and cannot be changed. In order to adjust the power output, the voltage applied must be controlled. This means that a transformer with on-load tapping is required to be able to control the heat generated in the pipeline for different operating modes.

2.2 Balancing system

Even though the load in DEH is single-phase, such large powers should not be supplied from a single-phase system. A Steinmetz balancing circuit is used to draw a single phase load from a three-phase network in a balanced manner [10].

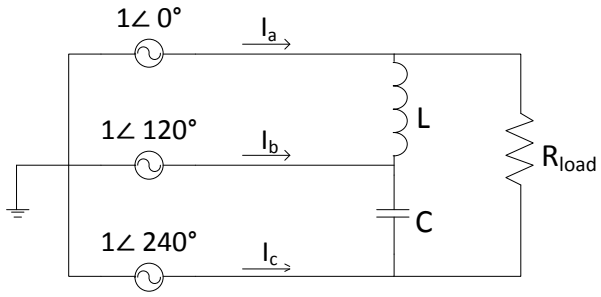

Figure 3: Generic three-to-single phase circuit

Figure 3 shows a simplified three-phase network supplying a single-phase load, representing the DEH load. Although a real DEH load will be highly inductive, the load is for simplicity assumed to be purely resisitive here. In a real DEH-system, there will be a large compensation unit making the load appear with a power factor close to unity, so this is a reasonable simplification for explanatory purposes. L and C are inductive and capacitive elements respectively, tuned to make the system draw a balanced three-phase current from the network. For a given load, the size of L and C can easily be determined:

$$I_a = \frac{1\angle 0° - 1\angle 240°}{R} - \frac{1\angle 120° - 1\angle 0°}{\omega L \angle 90°}$$

$$I_a = \frac{\sqrt{3}\angle 30°}{R} - \frac{\sqrt{3}\angle 60°}{\omega L}$$

If the power factor should be unity, I_a must be in phase with U_a. This yields

$$Im\{I_a\} = \frac{\sqrt{3}\sin 30°}{R} - \frac{\sqrt{3}\sin 60°}{\omega L} = 0$$

$$\omega L \sin 30° = R \sin 60°$$

$$\omega L = \sqrt{3}R \tag{2.1}$$

The value of C can be determined in a similar manner, yielding

$$\omega C = \frac{1}{\sqrt{3}R} \tag{2.2}$$

It should be noted that this derivation is only valid for a delta connected load. Connecting the load in star configuration would decrease the required value of L by a factor 3, and increase the required value of C by the same factor [11]. The phase sequence must also be as shown in Figure 3, as a reversed sequence would lead to asymmetric loading.

The balancing circuit is shown in Figure 4 alongside the compensation unit, and consists of capacitors and inductors connected between phases to ensure the 3-phase system is loaded in a symmetrical manner. In theory it is possible to achieve a load with power factor 1.0 as seen from the transformer secondary terminals, and to load the 3-phase supply network in a symmetrical style. A high power factor is important to keep the size and cost of the transformer as low as possible.

2.3 Compensation system

The capacitive unit used to improve the power factor may be connected either in series or parallel with the load. Connecting it in parallel will reduce the current drawn from the power source, while the source still needs to supply the full voltage required to feed the load. On the other hand, a series connected compensating unit will reduce the voltage required from the power supply, but the full load current will be drawn from the power supply. Assuming a unity power factor, the power source must either way only deliver the active power required by the load, regardless of the choice of connection.

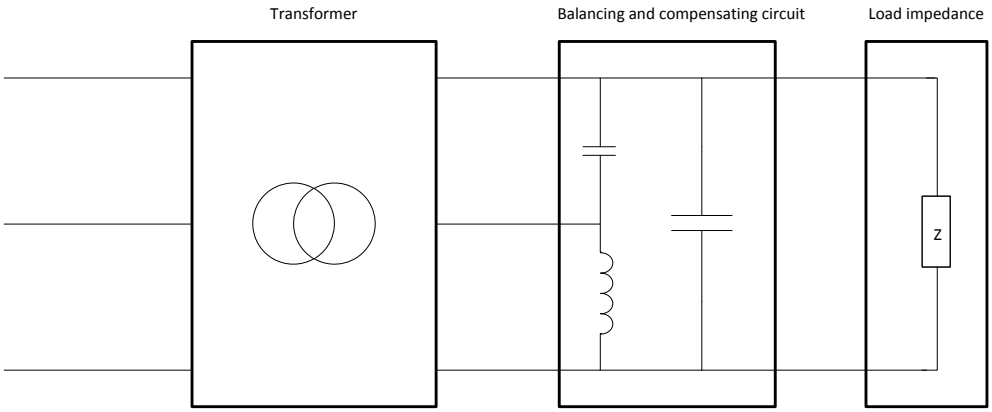

Figure 4: Circuit overview

Siemens have suggested using a series compensation strategy if a power electronic source is applied for a DEH system [10]. The required load current is not dependent on the length of the system, and the preferred converter can deliver the typical DEH currents in the range of 1000-1500A [12]. As DEH is applied to pipelines of increasing lengths, the increased power demand is met by increasing the voltage. The solution suggested by Siemens, consists of modular power cells with a given voltage rating. These are possible to series connect in order to obtain the desired voltage [10], thus offering increased flexibility.

2.4 System efficiency

The DEH systems in use, are supplied from either a 50Hz or 60Hz network. The operating frequency must be taken into consideration when designing the system, and the balancing and compensating circuit especially, as the impedance is frequency dependent. As the pipeline is grounded at both ends, the current can flow through either the pipeline or through water. At 50Hz, typically 40 % of the current flows through the water [4].

Tests have shown that the distance between the pipe surface and the piggyback cable also greatly affects the system efficiency. At 5cm distance, the efficiency was found to be approximately 60%, but it decreased to 45% if the distance was increased to 50cm [8].

Other values for system efficiency are obtained from [13], stating that as a rule of thumb there is 10 % loss in the cable, and 20 % loss in the sea water, making the total system efficiency approximately 70 %.

2.5 Pipeline

The pipelines come in a wide range of dimensions and properties. The diameter may be less than 10”[4], or it can be as high as 30”[8]. The pipelines can also be made from different materials, and with different material properties. DEH is usually not taken into consideration when selecting materials for the pipeline, and this may cause the pipelines to have unwanted properties from a DEH point of view. A typical issue that needs to be resolved, is that especially the magnetic permeability of the pipeline sections tends to differ within a wide range, even within the same batch [4].

The pipes can be made from different materials; carbon steel and Cr13 steel are among the most common. Typical material properties of these, used by SINTEF in their studies on DEH[13], are as given in Table 1.

Table 1: Pipeline material properties[14]

Material	Conductivity	Permeability
	σ [S/m]	μ_r [1]
Carbon steel	5.00E+06	400-800
Cr13 steel	1.43E+06	40-150

The thickness of the pipe walls may vary, but typical values are in the range of 11-25mm[4], [15].

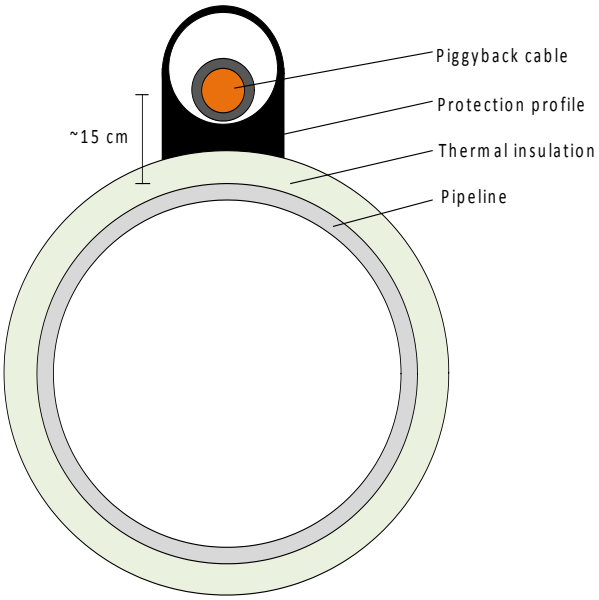

Figure 5: Cross-section of a typical pipeline and cable system[15].

2.6 Pipeline insulation

To avoid unnecessary heat dissipation into the ambient water, the pipeline must be equipped with thermal insulation. For insulated pipes on seabed, typical U-values are in the range of 3-7 W/m^{2}K, while it can be somewhat lower for buried flowlines [4]. Pipes may be partially buried, but pipe sections exposed to seawater still determine the heat requirement.

The power required by the system is proportional to the U-value, so improvements in insulation would make a big impact on the size of the system, both regarding investment cost, operation cost, and weight and size of the topside system. Statoil claim to have an insulation system with an U-value towards 2 W/m^{2}K under qualification [16].

The U-value can be further reduced by increasing the thickness of the insulation, but this is a tradeoff where material and transportation/installation costs increase with the thickness [17]. The thickness of the insulation may typically be in the range of 50-75mm [4], [15].

2.7 Current transfer zones and corrosion

As already stated, the piggyback cable is grounded in both ends of the pipeline. This is achieved using anodes made from aluminum [4]. It is mainly in these locations that current transfers from cable/pipe to sea water, and that the current in the water will have a non-parallel component with respect to the pipe. These sections, named current transfer zones and indicated as circles surrounding the pipe in Figure 2, must be of certain length and area, where typical lengths of the current transfer zones are 50 m [13]. This ensures a sufficient connection to the surrounding water, and avoids too high current densities where current transfers to water. Studies have shown that there will be no significant corrosion if the current density is kept below 240 A/m^2 [4].

2.8 Cable

The piggyback cable strapped to the pipe has to carry the total current in the system, while the return current flows through both sea water and the pipeline. Conventional subsea cables have a conductive screen to provide effective grounding of the outer semi-conducting layer, to maintain a low voltage over the cable protecting sheath [4]. As the conductive screen would have to be grounded in both ends to serve this purpose, it would become a conductive path causing the induced return currents to flow in the screen instead of the pipeline, thus reducing system efficiency. Using a screen with lower conductivity could reduce the unwanted currents flowing in the screen, but would cause excessive screen voltages [4].

One solution to this challenge, which has been implemented to the Tyrihans field, is to use a cable without screen, and instead use a semi-conductive outer sheath to continuously drain charging currents into the sea [4]. A model of this solution is found in Figure 6, where the piggyback cable is seen to lack the screen that the feeder and riser cables have.

Figure 6: Cross-section of cables used for the DEH installation at the Tyrihans field [18]

Regarding thermal considerations, the system current must be dimensioned to be able to heat the sections of the pipeline having the highest heat dissipation to the surroundings, which are the parts exposed to the seawater. Simultaneously, the cable can be covered by the seabed, providing unwanted thermal insulation of the cable. Therefore the cable must be selected with a sufficiently large cross-sectional area not to exceed the maximum operating temperature caused by this worst-case scenario, and a buried cable is hence the dimensional criteria for cable selection [13].

3 Converter selection

When selecting a power converter to feed the DEH load, there are several requirements and considerations that must be taken into account. Some are general for any converter, while others are specific for this given purpose. Some of the key requirements needed for the selection of the most suited converter for DEH application are identified below.

Two different power converter topologies have been suggested used for DEH purposes, the Perfect Harmony and the Multilevel Modular Converter (MMC). They are both multilevel converters, and they are presented in section 3.2 and 3.3. Both types of converters are used for 3-phase applications, but for these purposes they must be adapted to single-phase operation. Their suitability will be discussed based on the identified requirements.

3.1 Requirement specification

3.1.1 Voltage requirement

As already discussed, DEH is used for pipelines of increasing lengths. For a given power requirement [W/m], this means the required voltage will be proportional to the pipeline length. If a power converter solution is to be developed for DEH, it would be important to offer a solution that can be applied within a wide range of pipeline lengths. To this date, the highest applied voltage for a DEH system is for the 44 km long Tyrihans pipeline, which is operating at 23 kV [19]. Statoil DEH specialist Atle Børnes has suggested that DEH could be qualified for systems in excess of 100 km within few years [20]. If this is realized, voltage requirements will increase substantially.

The DEH load is highly inductive, with a power factor of typically 0.25-0.30 [10]. Consequently, large reactive powers will be drawn from the load. This reactive power will have to be supplied either by the converter or from a capacitive compensation unit. If the total apparent power is to be supplied from the converter, this unit will have to support both the full current and the full current required by the load. However, using a capacitor bank to supply the reactive power, the power converter need only supply the active power.

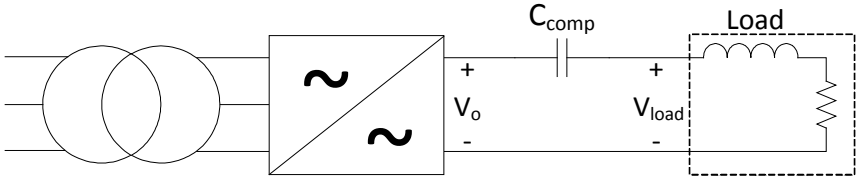

Figure 7: Simplified circuit diagram with series compensation

If a series compensation strategy is used, the output voltage V_o of the converter need only be V_{load} times the power factor, or in practice slightly more. This will allow high load voltages to be

supplied while keeping the converter output voltage at more modest levels. On a study performed by Siemens on a possible converter solution for DEH at the Njord platform, it was shown that a converter output voltage of 3.35 kV was sufficient to support a load voltage of 12.1 kV [10]. To enable the use of a power converter for DEH systems of increasing lengths without approaching exceedingly high converter output voltages, a series compensation strategy will be desirable.

While series compensation seems desirable in order to limit the required converter voltages, it may in practice be difficult to implement on DEH systems supplied from Floating Production, Storage and Offloading (FPSO) units. The FPSOs continuously realign to handle waves, but as the DEH cables should be held in a still position, they are typically located on a rotating platform. Current is supplied via slip rings that have got a limited current capacity. In order to reduce current over the slip rings, it may be required to use a parallel compensation unit located on the platform [12]. In such an event, the converter must support the full load voltage, but with a greatly reduced converter current.

3.1.2 Current requirements

The current required by a DEH load is not dependent on the length, as neither required power nor resistance per unit length are functions of system length. Consequently, load currents for various systems are within a narrower range than load voltages. However, there are some aspects that may impact the required load current. Larger pipeline diameters, or more precisely, a larger cross-sectional area of the pipeline, will reduce the per unit resistance, thus requiring a higher current for a given power requirement. Larger diameters may also lead to increased volumes to be heated and larger power dissipation to the surroundings, therefore adding to the power requirement. Furthermore, DEH may be installed retrofit on pipelines without thermal insulation, thus calling for substantially increased power and therefore also current.

The Ormen Lange pipeline has a retrofit DEH system prepared. This pipeline has both a large diameter (30”) and a lack of thermal insulation. Due to these factors, the required current will be very large, with figures ranging from 2600 A [20] to 3000 A [19]. In other installed DEH systems, currents have been in the range of 1100 A (8” pipeline) to 1640 A (18” pipeline) [19].

These values are current being fed to the load. For a series compensation strategy as discussed above, the converter will have to deliver the full current, while parallel compensation will require the load current times the power factor.

3.1.3 Frequency

In contrast to current DEH systems, which operate at fixed frequency, power converters may give an output frequency within a wide range. It has been suggested increasing operating frequency to increase the system efficiency, but simulations performed by the author indicated that no substantial efficiency increase was evident [21]. However, as no systems have been tested whilst operating at increased frequencies, no safe prediction on the influence on efficiency can be made. Higher frequencies would lead to increased load resistance and reactance, thus implying that a

higher voltage must be utilized. This effect will be opposed by the reduced current requirement due to the mentioned resistance increase, and possibly the increased efficiency.

There is at this stage no clear answer to how the frequency affects other parameters, but a converter solution should be able to operate at frequencies well beyond grid frequency. In the rest of this thesis, an output frequency of 75Hz has been used based on a best guess, but higher frequencies may also be utilized.

3.1.4 Modularity, flexibility and compactness

If a power converter is to be used for DEH purposes, then a modular system will be preferable for several reasons. A modular system means a system with standardized converter modules that can be adapted to different DEH loads by combining a suitable number of modules, thus allowing for components manufactured in high quantities. For long pipelines, that require higher voltages, one can stack several modules in series, adding their individual output voltages to form a high total voltage. For shorter systems, a lower number of modules can be used, as the voltage requirement is reduced.

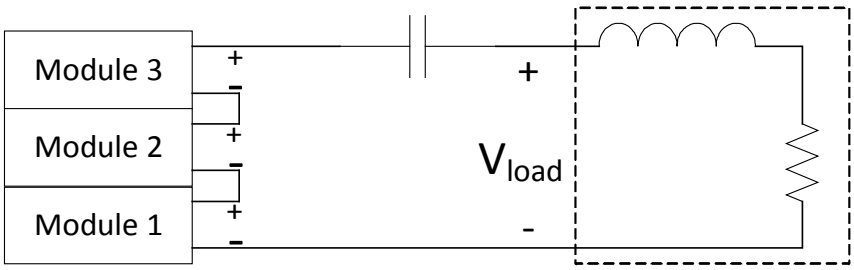

Figure 8: Example of 3 converter modules stacked to obtain higher voltage

DEH systems are usually supplied from an offshore installation, although pipelines to shore can indeed be fed from shore. There may be limited available space in offshore installations, and a compact solution where the converter is flexible in terms of location and arrangement is essential.

3.1.5 Reliability

Reliability has always been a key factor when selecting a system for nearly any application. In the offshore industry, this requirement is even stronger. The DEH system is a flow assurance method, and a failure of the DEH system can be very costly as it can cause a full stop of pipeline operation. A power converter for these purposes must therefore have a very high overall reliability. Factors to be considered are redundancy, low number of components, known technology and operating experience.

3.1.6 Losses

As discussed in Section 2.4, there are large losses involved with currents flowing in the sea water parallel to the pipe. These contribute to a low overall efficiency of DEH systems. Still, having a power source with a high efficiency is important. If the DEH solution is used for continuous

operation, then the aggregated energy losses in the converter may add up to considerable amounts, while this will be less of a concern if the DEH system is only applied during start/shut-down and plug removal. Independent of operating strategy, a cooling system with sufficient capacity must be installed in order to remove the generated heat and keep the temperature(s) at an acceptable level.

3.1.7 Load considerations

One of the most common applications for power converters is motor drives. Some motor drive applications require precise control of torque, speed and position, while other drives have less complex requirements in terms of degree of control [22].

The DEH load is a somewhat different load than electrical machines. It is a passive load with less complex requirements than drives applications. Although the load is passive, it is distributed over the full length of the DEH system. One should not expect any sudden load changes that require a quick dynamic response, with the only exception being a short circuit, in which case the solution must offer sufficient protection.

Since the DEH system forms a single-phase load, the active power consumption will pulsate at twice the operating frequency, as opposed to three-phase systems having constant power consumption. This may cause a need for extra energy storage in the converter solution or other measures to avoid unacceptable impact on the grid.

The preferred converter should not have any extra functionality that introduces unnecessary complexity and/or costs that could otherwise have been avoided.

Based on this, it is possible to summarize idealized desired features of a power converter for DEH applications, shown in Table 2.

Table 2: Desired features of a converter topology for DEH application

Type	Requirement	Typ. Value
Output voltage	Should be able to obtain high voltage for long systems	1-10 kV[1]
Output current	Sufficiently large to support high power requirements	1.5-2.5 kA[1]
Modularity	Should support standardized modules with high flexibility	
Reliability	Equal to or better than the passive solution	
Compactness	More compact than the passive solution	
Efficiency	Equal to or better than the passive solution	
Harmonics	Low impact on mains, low THD in output	

[1]Assuming series compensation

3.2 Perfect Harmony (PH)

The Perfect Harmony converter solution is a series connected H-bridge (SC-HB) converter delivered by Siemens [23]. It consists of individual low-voltage cells that can be stacked in series

to obtain the required output voltage. It is a medium-voltage converter with vast operating experience. An illustration of a cell with a diode rectifier is given in Figure 9. Each cell is capable of producing a voltage V_C of either $+V_{DC}$, 0 or $-V_{DC}$. In general, if *n* cells are connected in series they can produce (*2n+1*) switching levels per phase leg [24]. In a single-phase application such as DEH, this is also the number of voltage levels obtainable in the total output voltage. The peak voltage obtainable at the output will be $\hat{V} = n \cdot V_{DC}$.

If the PH is used as a single-phase inverter, this is achieved by removing two of the three legs shown in Figure 10, thus operating only a single leg. The number of switches in the inverter would then be

$$n_{switches,1} = 4 \cdot n_{cells} = 2 \cdot (n_{levels} - 1)\ ,\ n_{levels} = 3, 5, 7 \ldots \tag{3.1}$$

for the single-phase inverter.

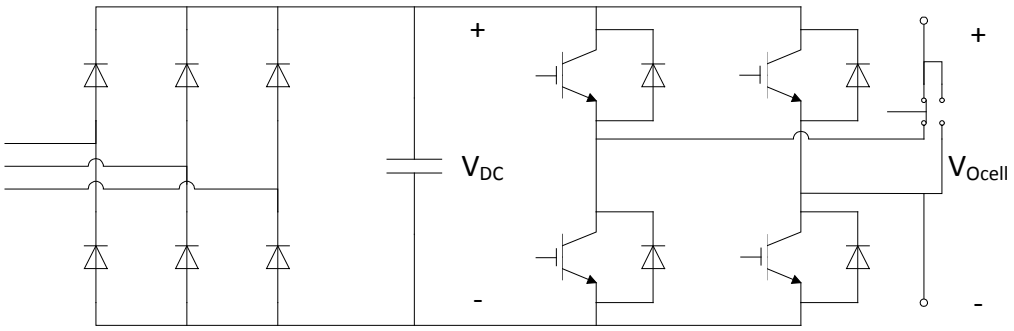

Figure 9: Perfect Harmony cell with diode rectifier and bypass switch

The PH offers redundancy by being able to bypass a cell if a cell fault should occur. The remaining *n-1* cells are then still able to continue operating with a voltage of $\hat{V} = (n-1)V_{DC}$.

3.2.1 Perfect Harmony transformer

A downside of the PH is that each inverter cell requires a separate isolated DC-source. This is achieved by using a special-purpose transformer designated for the task, that has got separate secondary windings for each cell [23]. An illustration of the transformer and cell arrangement for a 3-phase motor drive is given in Figure 10. In the figure, it is seen that the secondaries of the PH transformer are phase shifted with respect to each other, in order to form a multipulse action on the mains. According to [23], using a 18 to 36 pulse rectifier is the standard, depending on the cell number.

Although the transformer aids in keeping the influence on the power quality of the grid low, it is a custom made transformer designed for a given application, therefore being more expensive than standard transformers of comparable MVA rating. The transformer secondaries are three-phase 690 V supplies feeding the cell rectifier. As there are several of these low-voltage, high current

supplies, the PH transformer must be located as near the converter as possible to ensure a volume-efficient solution without excess cabling [25]. Such constraints on location is undesirable for offshore applications, where space is limited and it may be required to place different components in separate rooms.

The PH transformer also offers reduced flexibility. In the event that a converter solution is to be applied for DEH systems requiring a higher voltage rating, it is not possible to increase the cell number beyond the number of windings on the transformer once a PH transformer is installed. It will of course be possible to oversize the solution right from the start if usage on longer pipelines is anticipated in the future. If additional cells are introduced to increase the maximum possible output voltage, then this will also contribute to less harmonics in the output since the number of switching levels is increased.

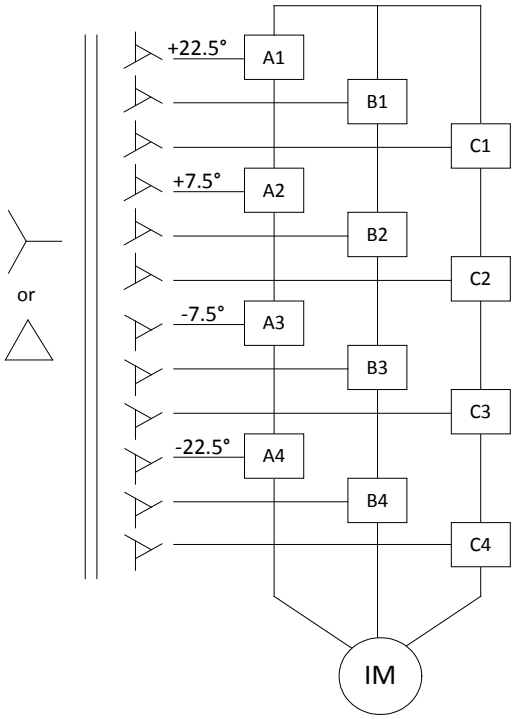

Figure 10: Transformer and cell structure of a 3-phase PH drive [23]

Standard 3-phase Perfect Harmony drives are available in ratings up to 13.2 kV and 1400 A [23] with the star configuration shown in Figure 10, corresponding to a phase voltage of 7.6 kV. Siemens have also suggested using the Perfect Harmony for DEH applications with higher current than the 1400 A mentioned above [10]. IGBTs with higher current ratings are available, as discussed in Section 3.4.

3.3 Modular Multilevel Converter (MMC)

The MMC is a multilevel converter proposed in the early 2000's. It is developed to offer a highly modular converter that can easily be scaled to meet a given power demand. MMC can be applied

for very high voltages. In 2010 Siemens' HVDC PLUS system using MMC technology was installed for the San Francisco Trans Bay cable, which operates at ±200 kV DC [26].

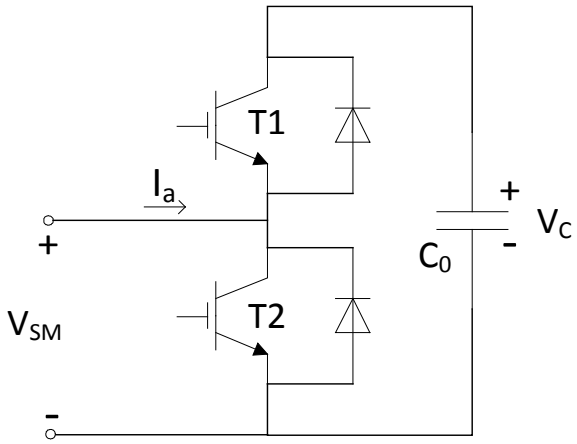

Figure 11: MMC submodule structure

The basic building block, from here on referred to as a submodule, of the MMC is shown in Figure 11. It is a simple structure consisting of two IGBT switches and one capacitor unit, and acts as a voltage source where the voltage V_{SM} can be controlled to be either 0 or V_c, depending on the switching state. Table 3 shows an overview of the voltage and charge/discharge of the capacitor that corresponds to the different states of the sub module.

Table 3: Switching states and corresponding voltage of submodule

T1	T2	V_{SM}	I_a	dV_c/dt
On	Off	Vc	>0	>0
On	Off	Vc	<0	<0
Off	On	0	>0	0
Off	On	0	<0	0

By connecting multiple sub modules in series and controlling their voltages individually, one is able to obtain an overall output voltage that can be adjusted in steps. The MMC concept requires that each phase leg has two arms with the same number of modules. The sum of the voltages in the two leg arms must always be equal to the voltage V_{DC}.

The MMC was initially developed as a three-phase converter [27] but can also be used as a single-phase converter. The single-phase converter can be created by keeping either one or two of the three legs found in a three-phase converter. The submodules, as illustrated in Figure 11, are only able to produce a positive voltage in addition to the zero voltage level, they are not able to reverse the voltage polarity to the output. Hence, operation with only one leg would require connection to a DC-link midpoint and twice as high DC-voltage as operation with two legs, where the load voltage is the difference between the two arm voltages. Double DC-voltage would require a series connection of twice as many modules compared to the two-leg solution, and the amount of

components and switching levels would therefore be the same for the two solutions. The two leg solution is therefore the only alternative evaluated further. A model of a single phase inverter with n submodules per phase arm is shown in Figure 12.

The number of switches in the single-phase MMC inverter is

$$n_{switches,1} = 8 \cdot n_{sm,arm} = 4 \cdot (n_{levels} - 1)\,, \qquad n_{levels} = 5, 7, 9 \ldots \tag{3.2}$$

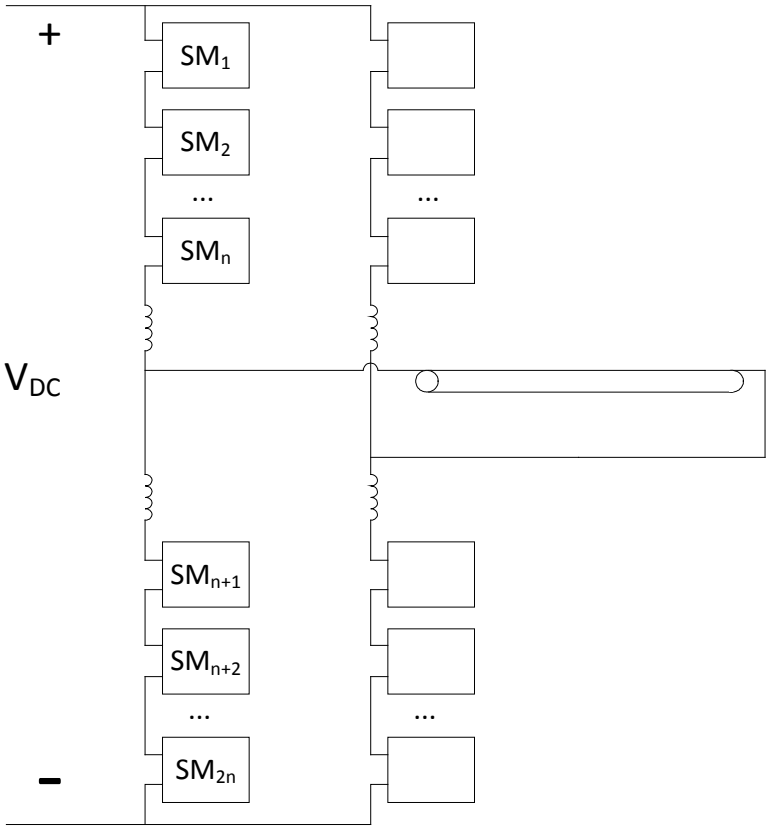

Figure 12: MMC single phase inverter with DEH load

Prior to operation, the submodule capacitors must be charged to their average value in order to avoid a very large inrush current. The MMC topology allows for such precharge directly from the DC-bus, thus avoiding the use of an external power source [28]. Adding an appropriately dimensioned charging resistor in each leg, the submodule capacitors can be charged one at a time, while keeping all other submodules short circuited by controlling the internal switches. The charging resistor is bypassed in normal operation. A similar way of de-energizing the submodules is also described in [28]. The procedures described are suited for both three-phase and single-phase inverters.

It is possible to continue operation of the MMC in the event of a fault in a sub module. The faulty module can be bypassed without using mechanical switches, and the remaining n-1 modules may continue to operate [27]. This would cause the DC-link voltage V_{DC} to be shared between the remaining submodules. In order to avoid voltage overload in such an event, all

submodules must be rated for operation with n-1 module. The alternative would be to reduce the DC-link voltage, given a controlled rectifier is used, but this would consequently reduce the maximum output voltage and the power capability.

The MMC bases its inverter operation on a single DC-voltage source, as opposed to the Perfect Harmony, which requiring several isolated DC sources. For DEH purposes, reversible power flow is not an issue. The DC voltage can thus be obtained from standard rectification solutions, with DC-link voltage control and low impact on mains as the key requirements. It is also possible to operate several inverters from a common DC-bus [29], either to feed multiple DEH-loads or to combine the DEH with one or more motor drives.

It is worth noting that the MMC topology makes the central DC-link capacitor dispensable, as the capacitors are instead distributed within the different sub modules. This reduces the risk of component damage in the event of a capacitor short circuit [27]. Furthermore, as shown in Figure 12, each arm contains an inductor in order to limit circulating currents. These inductors will also limit the short-circuit current. The circulating currents and the arm inductor are discussed further in section 5.3.5.

3.4 Evaluation of the two proposed topologies

Both converter types seem like feasible alternatives for DEH purposes. In terms of voltage, both converters will be able to support typical voltages required in a DEH system, assuming a series compensation strategy can be utilized as discussed above. However, the MMC topology has been used within a wider voltage range than the Perfect Harmony, which may favor the MMC for long pipelines or where series compensation is not possible. At high voltage levels, the Perfect Harmony may require a step-up transformer at the converter output, thus adding undesirable weight and volume to the system.

For both converters the current capacity is only a question of available semiconductor technology, but their difference in topology gives certain differences. There are available IGBT modules with sufficient current ratings to support the full load current of typical DEH loads for pipelines with thermal insulation, with modules both rated at 3.3 kV, 1500 A and 1.7 kV, 3600 A [30]. However, the full current rating of the IGBT should not be utilized. The MMC has a higher number of switches than the PH, and thus the stress on the individual IGBTs is reduced. This will favor the MMC in DEH systems where a large output current is needed, given that series compensation is preferred. While most DEH loads currently installed operate in the range 1000-1500 A, the Ormen Lange pipeline is installed without thermal insulation, and require a load current of 2600-3000 A. For a pipeline like Ormen Lange, a parallel compensation strategy would require a terminal voltage of 23 kV [19], this way making the PH unsuited regardless of compensation strategy.

Both converter topologies are modular, as they enable stacking of several modules to obtain the desired output voltage. It is therefore possible to standardize converter units of both types. However, the special purpose transformer required by the PH is a feature not required by the MMC, which can utilize more standard front end devices. While the PH transformer must be located near the converter cells, an input transformer for the MMC has no such requirements. Thus, the MMC offers better flexibility than the PH.

To the author's knowledge, no power converter has currently been used for DEH, and regardless of topology selection, the field of application will be new. However, the PH is a widely used converter topology with proven performance in motor drives applications, and it has been available on the market since 1994 [31]. The MMC is a more recent development [27], and therefore does not have the same amount of operating experience, although the different components used in the MMC are well known. Both converter types offer redundancy by enabling bypassing of a module should a fault occur. They also both have distributed capacitors, meaning they do not have a central energy storage in the DC-link but instead have the capacitors distributed in the cells/submodules. This helps to reduce the consequences of a short circuit, as the cells or submodules can be controlled by switching.

Any kind of converter solution will introduce some harmonics to a system. The challenge of keeping harmonics sufficiently low will be more demanding than for three-phase converters of the same topologies. However, by introducing appropriate measures, both converter topologies should be able to keep grid harmonics at an acceptable level. The PH and its special transformer utilizes 18-pulse rectification as a minimum, and claims to have very low impact on the mains [23]. The DC voltage required by the MMC inverter can be obtained in any way preferable, and so it should be possible to select a rectification solution having sufficiently low impact on the mains. In terms of output power quality, the fact that both converters are multilevel types suggests they will be able to produce output voltages with a shape approximating a sinusoidal waveform, thus keeping harmonics low. As shown in section 4.3.2, the output waveform will be closer to sinusoidal as the number of modules and switching levels increases.

3.4.1 Choice of topology

Based on the evaluation of the two topologies, it is clear that both topologies are capable of supplying a DEH load. The Perfect Harmony has a more comprehensive operating experience than the MMC, but the MMC is also built from known components. Regardless of converter choice, challenges related to harmonics on grid must be resolved. The single-phase converters will generate significant amounts of 2^{nd} harmonic oscillations compared to their three-phase relatives.

Table 4: Summary of single-phase converter properties

Converter	PH	MMC
Voltage ratings	Good	Very good
Current ratings	Good	Very good
Modularity/Flexibility	Good	Very good
Reliability	Very good	Good
Harmonics	Medium	Medium

It is shown that the MMC can achieve both higher voltage and current ratings than the Perfect Harmony. The Perfect Harmony is capable of supplying loads in the range seen on most present systems, but DEH is believed to be applied to increasingly larger pipeline systems in the future [20]. This will favor the MMC, which also is more flexible in terms of preferred compensation strategy, due to the extended operating range. Adding the increased modularity and flexibility of the MMC, it seems like the most suitable topology in order to develop a solution that can easily be adapted and applied to DEH loads within a wide range.

4 Converter simulation model

In order to simulate a DEH system and converter performance, a simulation model has been constructed in MATLAB Simulink. The model is built from scratch, as this makes it possible to create a control system specially designed for DEH purposes. Further, building a model from scratch also gives a more thorough understanding of the converter operating principles. The converter simulation model is the author's own work, with the only exception being the converter submodule block, copied from [32].

4.1 Basic converter structure

In Figure 13, the ground level of the simulation model is shown. The model is built with 6 submodules in each leg arm, a choice that is justified in Section 5.3.1. Each leg arm also includes a series RL-branch, where the inductance can be adjusted to reduce the circulating currents in the converter leg. The resistance in a leg arm is ideally zero, but it is included in the model to allow for simple inclusion of non-zero values if desirable. There is no central DC-link capacitor, as the capacitance in the DC-link is contained within the submodules. Not shown in the figure are two different filters applied on the DC-link, this is discussed in section 5.4.

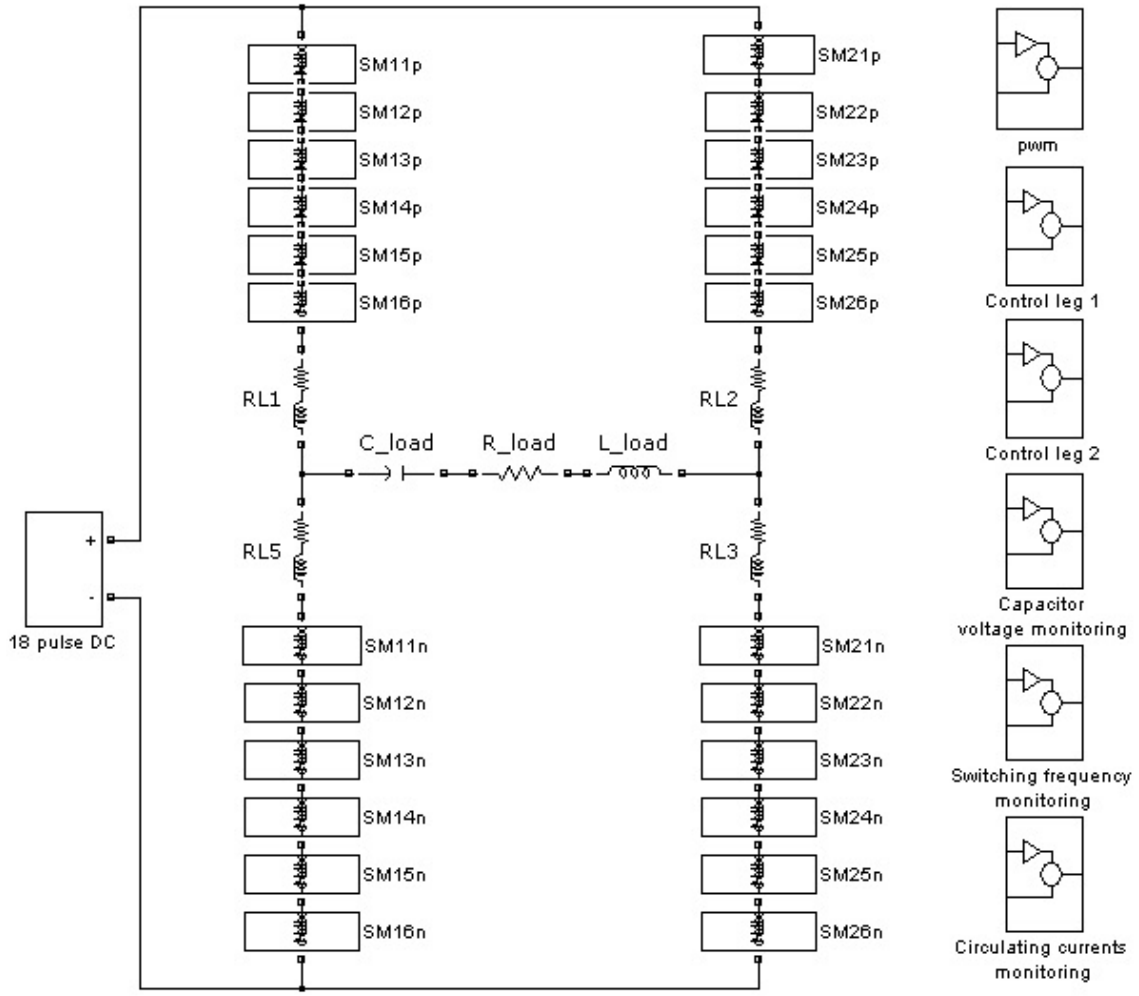

Figure 13: Simulation model ground level

Figure 13 also shows several subsystems on the right hand side. The first subsystem generates the PWM signal, while the two next subsystems uses these signals to control and execute the switching in the two legs. The 3 bottommost subsystems are virtual, meaning they do not affect the system performance. They are solely included to give a quick overview of system state throughout simulation studies.

4.1.1 Load modeling

The load, including the pipeline, cables and the compensating unit, is modeled as a series RLC-load with merged parameters. The resistive and inductive components are mainly found distributed along the length of the pipeline and piggyback cable system. Assuming an absence of distributed capacitance along the load, an assumption discussed below, the resistive and inductive components can safely be lumped together.

The capacitive component is primarily a discrete component found topside in the compensating unit. What the model fails to include, is the distributed capacitance found in the cables. The feeder and riser cables will contribute with distributed capacitances, but these cables are of limited length, as they only extend from the topside supply to the near end of the pipeline [33]. The piggyback cable extends as far as the pipeline but is sometimes made without an outer screen [4]. A single phase cable without an outer screen will have a reduced capacitance [34] and therefore not contribute as much to the overall system capacitance as more conventional cables would.

This way of modeling the load is therefore a simplification but should not be a source of large errors in the simulations. If a more detailed load model is desired, one could consider modeling the cables using a π-model, as described in detail in [35]. More detailed knowledge of cable length and parameters is then a prerequisite. In this model, the load is simply dimensioned by setting an active power requirement at a given current, with a typical power factor for a DEH system. The capacitive parameter is then set to compensate the load to give a unity power factor as seen from the converter. In the simulation model, the compensating capacitance is, by default, changing with the frequency to maintain the unity power factor regardless of chosen output frequency.

4.1.2 Converter submodule modeling

In Figure 14, the submodule used to build the converter is shown. The submodules are implemented in the same way as in [32]. Ideal switches instead of IGBTs contribute to reduced simulation time, while at the same time maintaining the required accuracy[36].

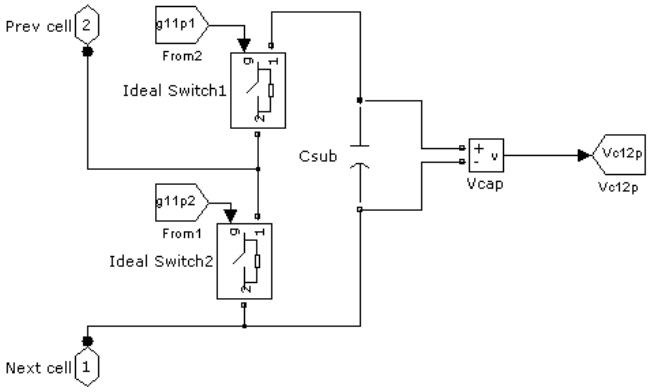

Figure 14: Model of converter submodule

In addition to the power components, the submodules include capacitor voltage measurement, which is necessary to achieve controlled voltage balancing. Each leg arm also includes a current measurement. The direction of the current is required as input to the switching algorithm.

4.2 Converter control system

The MMC model has a control system specially designed for DEH purposes. In many ways, the DEH system represents a simpler system than i.e. motor drives, which is a far more common application for power converters. The DEH load is passive and can be regarded to be constant. The control system of the converter should ensure proper operation in all operating scenarios, but should at the same time avoid unnecessary complexity required by more sophisticated loads. Protection and control required to operate the converter with a disconnected submodule has not been implemented.

4.2.1 Current control

The heating requirement of the subsea pipeline sets the requirement for current delivered by the converter, either directly through setting a target current or derived from a given active power requirement. If the DEH load is known, and assumed constant, it will be possible to operate the converter without a current control loop.

As already discussed, the DEH load is passive and essentially constant. However, the exact load impedance may be unknown, or the load impedance may vary slightly over time, as conductor resistance in general is temperature dependent [34]. A change in resistance may lead to different current distribution in the pipeline and can also affect system inductance. No data on load impedance temperature dependency is available, but a current control loop has been implemented into the control system to account for such variations. The heating requirement depends on whether the system is used to melt a hydrate plug or for continuous hydrate prevention at lower power, as discussed in section 2.1. The current controller facilitates simple change in developed heat by adjusting the current reference, in order to switch between these operating modes.

The current is controlled by adjusting the modulation index, m_a, of the reference signal used in the PWM-generator.

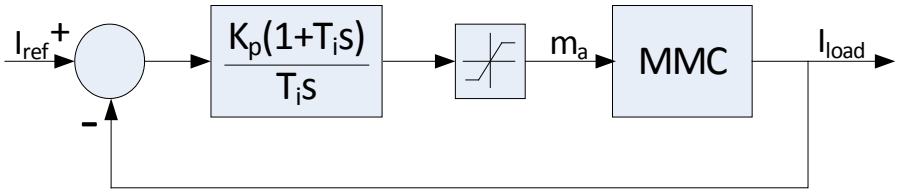

Figure 15: Converter current control loop

As seen in Figure 15, a PI-controller is used to minimize the deviation between the reference current and the load current. The integrator term is included to avoid a steady-state deviation from the reference [37], while the saturation block ensures the modulation index does not exceed a specified value. This value is normally set to 1 to avoid overmodulation, which is discussed in section 4.3..

The PI-controller also includes anti-windup behaviour of the integrator term. It ensures that the input to the integrator term is grounded if the controller output reaches its limit, thus helping to preserve stability [22]. The parameters used in the PI-controller are

$$K_p = 0.0024\,,\; T_i = 0.06s$$

and the resulting response to a step in the reference is shown in Figure 16.

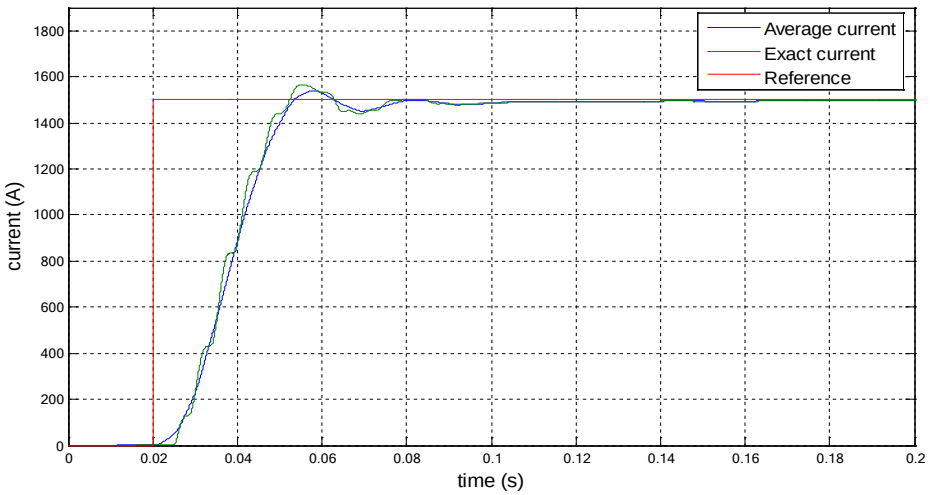

Figure 16: Current response at f_{ac}=90 Hz

The parameters are obtained by using the Good Gain method, which is described in [38]. A detailed description of the tuning procedure is found in Appendix A.

4.2.2 Submodule voltage monitoring and control

As explained in section 3.3, each submodule can output a voltage of either 0 or V_c, the submodule capacitor voltage. During operation, the capacitor voltage will vary as described in

Table 3. Proper operation of the converter requires the voltages of the submodule capacitors to be balanced. In order to achieve this, all submodule capacitor voltages are monitored.

In the control system, two different voltage balancing algorithms have been implemented, where both are efficient in making sure the capacitor voltages do not drift off. Still, they have some different attributes. The inputs to the algorithms are the submodule capacitor voltages, gate signals applied in the previous switching period and the current direction in the arm. The number of submodules, N_{on}, to be ON ($V_{SM}=V_C$) in the new state is also taken as input. The MATLAB-code written for the algorithms is found in Appendix F.

Normal switching algorithm

The normal algorithm is explained in [27]. When the current through the arm is positive, the N_{ON} modules with the lowest capacitor voltages are switched ON, and these capacitors will be charging, while the modules kept OFF have constant voltages in the same interval. When the current through the arm is negative, the N_{ON} modules with the highest voltages are switched ON, thereby discharging the corresponding capacitors. In this manner the capacitor voltages are continuously balanced.

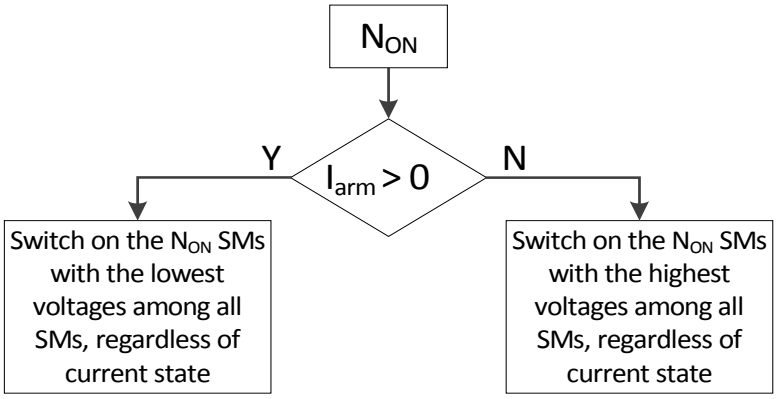

Figure 17: Flowchart of normal switching algorithm

At all times, the modules with lowest voltages or the modules with the highest voltages are discharging. The normal algorithm therefore causes a very good voltage balancing. However, one might experience that 2 modules are switched ON and 1 module is switched OFF in order to achieve a net increase in N_{ON} of 1, depending on the capacitor voltages. Although this ensures the best possible voltage balancing, it also causes higher switching frequencies that result in higher switching losses.

Reduced switching frequency algorithm

The reduced switching frequency (RSF) algorithm is proposed in [39]. The means of voltage balancing is the same as for the normal algorithm, however the selection criteria for which

modules to switch is different. In the RSF algorithm, if additional submodules are to be switched ON, the submodules already ON will remain in their given state, while the normal balancing algorithm is only applied to the modules currently in the OFF state. Similarly, if the number of modules ON is to be reduced, the normal balancing algorithm is only applied to submodules currently in the ON state.

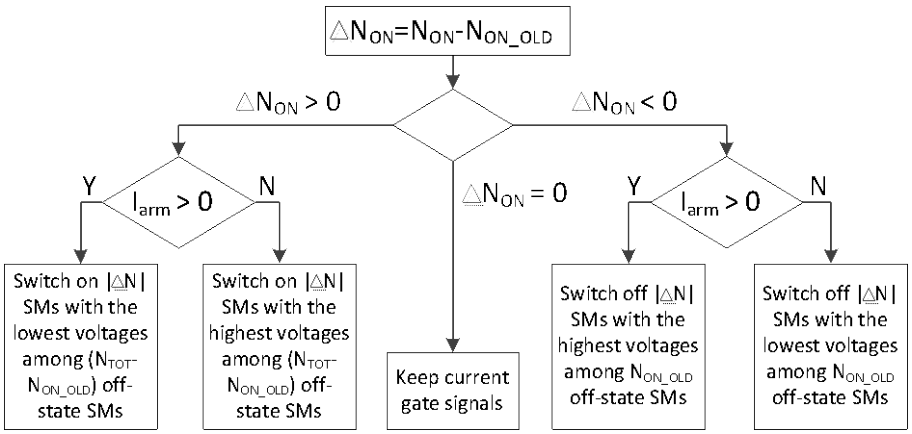

Figure 18: Reduced switching frequency algorithm

Effectively, the RSF algorithm avoids switching of more than 1 module in each arm at a time, thus reducing the switching frequency and thereby also the switching losses. The trade-off is that the submodule capacitor voltages may deviate more from each other than when using the normal algorithm.

Algorithm selector

As argued, both switching algorithms have desirable features. An algorithm selector has been implemented into the model in order to enable good voltage balancing while also keeping the resulting switching frequency at a low level, as shown in Figure 19.

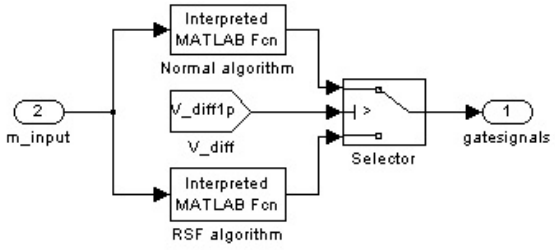

Figure 19: Switching algorithm selector

By default, the RSF algorithm is run when a module is to be turned either ON or OFF. V_diff in the figure gives the voltage difference between the most charged and the least charged submodule capacitor in a leg arm. Should this difference become larger than a set tolerance limit, the normal algorithm will be executed instead, thus giving improved voltage balancing. Due to this, the normal algorithm is only executed when required in order to maintain sufficient voltage balancing, while the resulting switching frequency can be kept low. Setting the tolerance limit to

0 will cause the normal algorithm to be executed every time, while larger values increasingly will favor the RSF algorithm. The tolerance limit can be set individually for each leg arm, thus enabling easy comparison of the effect of different settings.

4.3 Pulse-Width-Modulation

In the inverter, a DC-voltage is to be converted into a sinusoidal voltage. For multilevel converters, a common modulation strategy is the level-shifted carrier based Pulse-Width-Modulation (PWM) scheme, which is a continuation of the PWM for two-level-inverters [24].

4.3.1 Two- and three level PWM

In carrier-based PWM, a low-frequency target reference waveform, V_{ref}, is compared to a high-frequency carrier waveform, V_{tri}. For a two- or three-level inverter, the inverter leg is switched to the upper DC-rail when the reference waveform is greater than the carrier waveform, and to the lower DC-rail if the reference is smaller than the carrier waveform [24].

The reference waveform has the general form

$$v_{az}^{*} = m_a \cos(\omega t + \theta_0) \tag{4.1}$$

where

- $m_a = \hat{V}_{o1}/V_d$ = modulation index, a normalized output voltage magnitude
- ω = output frequency [rad/sec]
- θ_0 = output phase

The carrier waveform is usually triangular. In two-level inverters, the two converter legs are switched simultaneously, termed bipolar switching, and therefore they only need a single reference signal. The terminal voltage V_{ab} of a two-level inverter is either V_d or $-V_d$. If the converter legs are controlled individually, called unipolar switching, two reference signals must be applied. If a unipolar switching scheme is applied, the output voltage may either be V_d, 0 or $-V_d$, therefore being a three-level inverter. The 0 voltage level is possible since the two legs now are allowed to be at the same potential simultaneously.

When using unipolar switching in single phase inverters, the modulation frequency, $m_f = \frac{f_{tri}}{f_{ref}}$, should be an even multiple of the reference frequency in order to cancel low-order harmonic content [40].

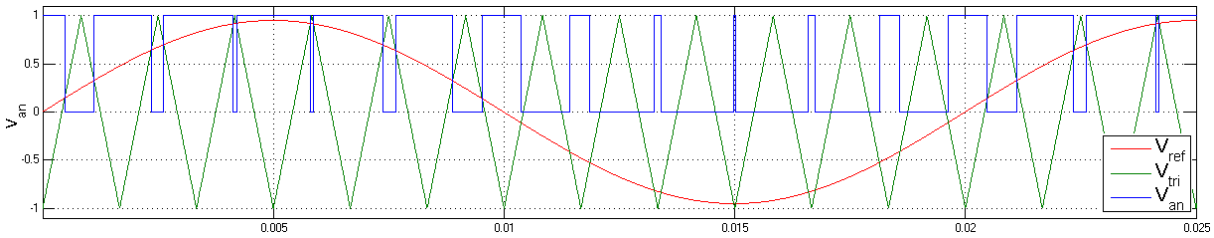

Figure 20: Pulse-Width-Modulation of one inverter leg, m_a=0.95, m_f = 12

Figure 20 illustrates the basics of PWM for one leg of a three-level inverter. One can see how the leg output voltage, V_{an}, changes with the reference and triangular signals. V_{an} has the same frequency and phase as the reference signal, and its fundamental harmonic has an amplitude of

$$\hat{V}_{an1} = 0.5 m_a \cdot V_d \tag{4.2}$$

where V_d is the DC-link voltage. Since the reference signal of phase b is shifted 180° from the phase a reference signal, the fundamental harmonic of the terminal output voltage of a single-phase converter, V_{ab}, is [40]:

$$V_{ab} = V_{an} - V_{bn} = 2V_{an} = m_a \cdot V_d \cos \omega t \,, \quad 0 \leq m_a \leq 1 \tag{4.3}$$

From equation (4.3) it is seen that the output voltage is proportional to the modulation index m_a. To ensure a good utilization of the DC-voltage, operating the converter with a high modulation index is important.

If the modulation index m_a exceeds unity, referred to as overmodulation, the output voltage will no longer increase proportionally to m_a. Instead, it starts to saturate and eventually reaches square-wave switching, which is not described here. Overmodulation enables a better utilization of the DC-voltage, but at the expense of increased harmonic content in the output [40].

4.3.2 Multilevel switching

Multilevel converters are inverters where the number of possible voltage levels in the terminal output is increased beyond the two- or three levels described above. Multiple voltage levels are achieved by having multiple cells connected in series. With proper control of the cell's output voltages, one is able to obtain an output voltage closer to the reference than for two- or three level inverters.

Multilevel inverters require a somewhat more advanced PWM than what is described in the section above, but the method is derived from two- and three-level PWM. One of the PWM strategies used, is the carrier based level-shifted PWM using phase disposition (PD) [24]. Instead of using one carrier signal as in a two- or three-level inverter, L_a-1 triangular carriers are used, where L_a is the number of voltage levels obtainable in one inverter leg. These carriers are level

shifted so they create contiguous bands in the range $-(L_a - 1)/2$ to $(L_a - 1)/2$. Each carrier then corresponds to the switching of one module in the multilevel inverter leg. If all carriers are in phase with each other, this is called phase disposition (PD).

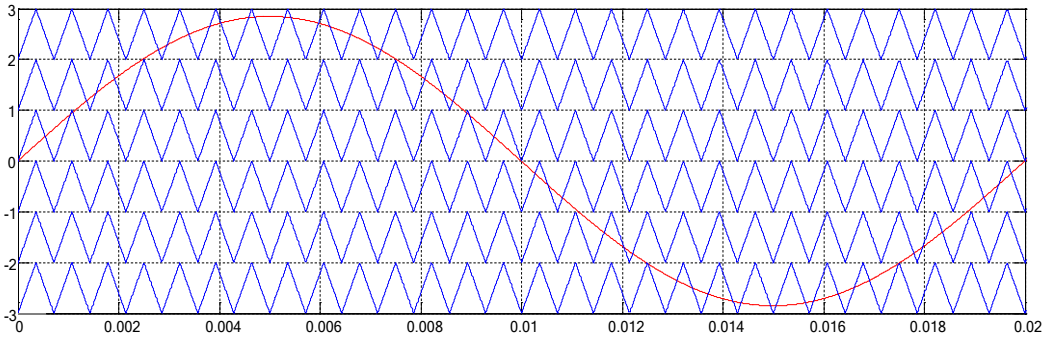

Figure 21: Level-shifted PWM using PD for L_a=7, m_a=0.95

In Figure 21, the described PWM algorithm is visualized for an inverter leg capable of producing 7 different voltage levels. The amplitude of the reference signal is no longer m_a, but instead m_a multiplied with a factor $(L_a - 1)/2$.

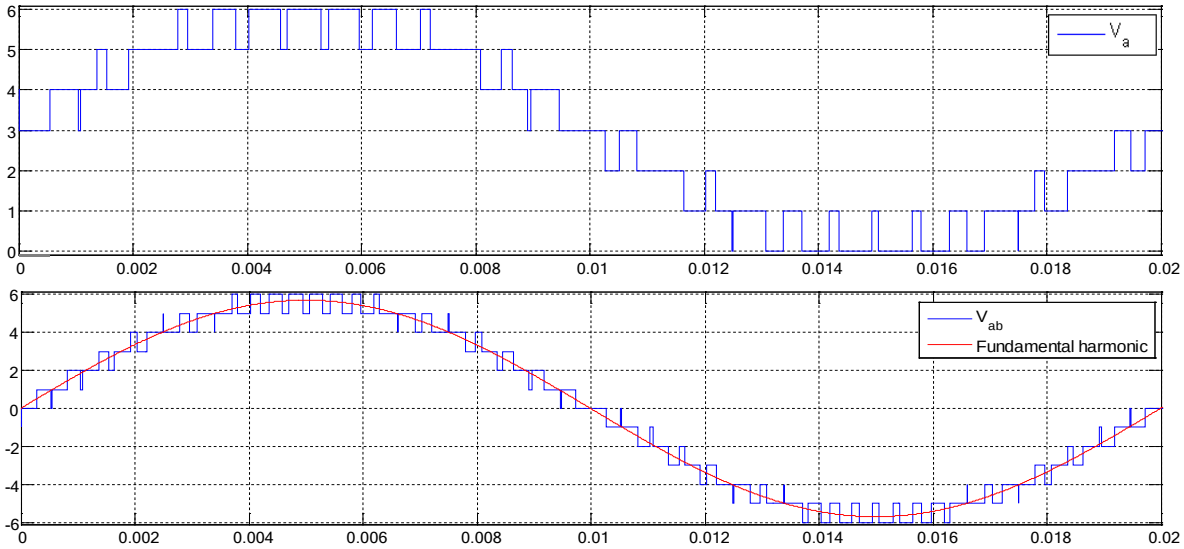

Figure 22: Resulting switching pattern using the PWM in Figure 21

In Figure 22, the resulting, idealized voltages from the discussed PWM scheme are shown. The line-to-line voltage V_{ab} has twice the amplitude, voltage steps and resulting switching frequency of the phase voltage V_a. The figure illustrates some of the features of multilevel converters:

- More sinusoidal output voltage reduces harmonic content
- The DC-voltage is switched in multiple steps, reducing $\frac{dV}{dt}$
- Reduced need for filters due to more sinusoidal output
- A lower switching frequency can be used, reducing switching losses

4.3.3 Multilevel switching using low modulation index

The level-shifted PWM-scheme used has been illustrated using a high modulation index, m_a=0.95. If the reference signal amplitude is reduced until it fails to pass through all carrier bands in one fundamental period, then the inverter will operate with a reduced number of voltage levels, thus reducing performance [24]. In addition, a low modulation factor causes a poor utilization of the DC-voltage. Operating at a low modulation factor is therefore generally not desirable. The minimum modulation index m_a required to maintain a certain number of voltage levels in an inverter leg can be expressed as:

$$m_a > 1 - \frac{(n+2)}{(L_a-1)} \ , \ \text{n} = [0, 2, 4\ldots] \tag{4.4}$$

Where

- L_a = the maximum number of voltage levels obtainable in one inverter leg.
- n = the reduction in number of voltage levels in one inverter leg. For m_a=1, n=0.

The reduction in voltage levels in equation (4.4) is referred to each leg. For most converter topologies, including the single-phase MMC, the number of voltage levels in the line-to-line voltage is

$$L_{ab} = 2L_a - 1 \tag{4.5}$$

This means the number of levels in the output voltage is reduced in steps of 4 if m_a is reduced beyond threshold values obtained in equation (4.4). By reducing m_a sufficiently, the inverter will eventually degrade to a three-level inverter. Although a reduced m_a as discussed will have some obvious disadvantages, the fundamental harmonic will still have a value equal to the reference, and the voltage stress on each cell/module in the inverter is unchanged.

4.3.4 Other modulation alternatives

The PWM strategy presented is only one way of achieving the modulation of an inverter. Other strategies with various advantages and disadvantages in different applications are also available. It is worth noting that quite a few modulation strategies frequently used in three-phase inverters are unsuited for use with single-phase inverters [24].

4.4 PWM algorithm

The PWM subsystem shown in Figure 13 generates the switching signals taken as input by the Control subsystems. It uses a level-shifted pulse-width modulation strategy, which is explained further in section 4.3. The PWM subsystem does only determine the number of modules to be in the ON-state in any given interval. The determination of which modules to switch is performed by the control subsystem for each leg, based on submodule capacitor voltages and direction of current. The PWM subsystem also outputs a trigger signal each time a switching is set to occur in

order to ensure the switching algorithm is only executed whenever a switching is set to occur, thus reducing simulation time. The legs are controlled independently of each other, so-called unipolar switching, and each leg therefore has its own PWM signal.

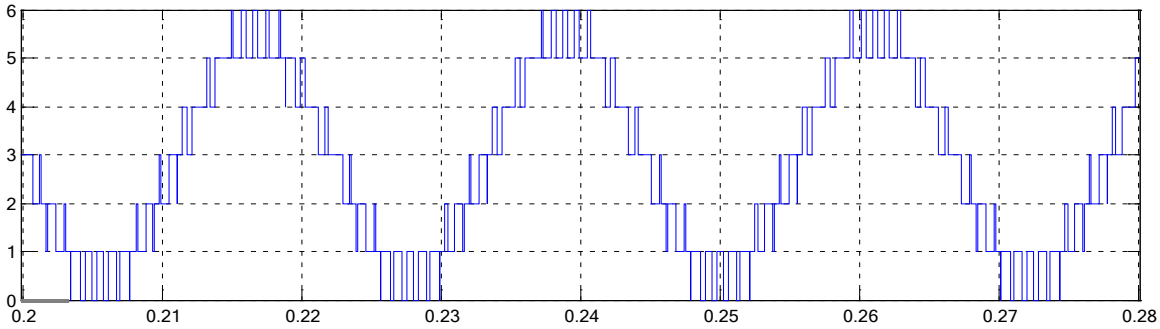

Figure 23: Example of output from PWM subsystem

5 Case study of a DEH converter

The feasibility of using a power converter solution for direct electrical heating is considered in the following. The study considers a generic scenario with specifications, requirements and ratings set to typical values, in order to reflect a real case as far as possible.

5.1 Grid and rectification solution

The DC-voltage required by the MMC is delivered through an 18-pulse diode rectifier with phase-shifting transformers fed from an 11 kV grid. The transformers also serve the purpose of isolating the converter from the grid. This is vital due to the DEH concept requiring one of the converter terminals to be connected directly to ground.

Table 5: Grid data

Rated power	15	MVA
Voltage	11	kV
frequency	50	Hz
X_d"	0.15	pu
X/R	15	

The rated power of 15 MVA is set to represent a fairly modest sized platform generator supplying power to compressor loads. If the converter influence on a conservatively dimensioned grid is found to be within specified limits, then it will also be able to operate on larger grids. Harmonic content is discussed further in section 5.5. The values of X_d" and R are typical values for synchronous generators of the given size [25], [41].

Table 6: Transformer data

Rated power	1.5	MVA
Z_t	0.07	pu
R_t	0.01	pu

Three phase-shifting transformers are required when using an 18-pulse rectifier. Each of them are modeled according to Table 6. The magnetizing current of the transformers is ignored throughout the simulations. Transformers of the given rated power will have an approximate weight of 3100 kg each [42]. No voltage rating of the transformers is specified here, as the turns ratio is adjusted depending on the required DC-link voltage. The 18-pulse rectifier is modeled as 3 series connected ideal full-bridge diode rectifiers. The average DC-link voltage will thus be [40]

$$V_{dc} = 3 \cdot 1.35 V_{LL} \tag{5.1}$$

Where

- V_{LL} = secondary transformer voltage

5.2 Load data

The load parameters used are typical values found in DEH systems, and are based on the system description in Section 2.

Table 7: Load data for a typical system

Parameter	Value	Unit
Required load current[1]	1500	[A]
Power factor [1]	0.25	inductive
Cable length	25	[km]
Power requirement	160	[W/m]
Active power requirement	4	[MW]
Apparent power requirement[1]	16	[MVA]
Load voltage[1]	10.7	[kV]

[1]Value at 50 Hz

The study is based on a MMC mainly supplying the active power, while the reactive power is supplied from a series connected compensating unit. As a consequence of this, the converter must be dimensioned to handle the full load current but at a greatly reduced voltage compared to the load voltage, as explained in section 2.3.

5.2.1 Load power factor estimation

A power factor of 0.25 has been stated as a typical value. This value is obtained from systems already in operation and is therefore obtained at grid frequency. Figure 24 shows how the power factor may change as the frequency is varied. Two load models have been considered used; a simplistic case where the load resistance has been assumed constant and a more realistic case where the resistance increases with frequency due to factors such as the skin effect. The frequency dependent resistance is described as

$$R = (0.01125f + 0.439) \cdot R_{50} \tag{5.2}$$

Where

- R_{50} = load resistance at 50 Hz

The derivation of the expression is found in Appendix B and is based on data found in a study performed during the specialization project [21]. Using the two different resistances yields very different power factors at higher frequencies. The varying resistance model has been used in the simulations, as it is believed to improve the accuracy in the simulations.

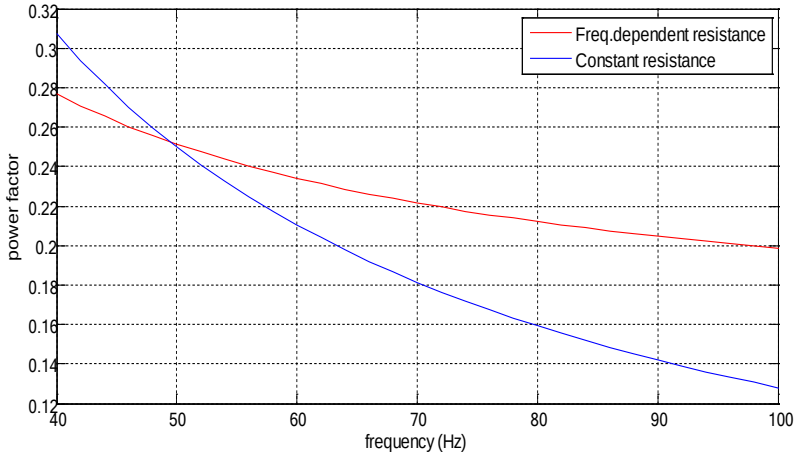

Figure 24: Load power factor vs. frequency

The figure shows that the power factor will be reduced if a higher output frequency is utilized. This is due to the increased load reactance. To the author's knowledge, DEH systems have not been tested or operated at frequencies other than grid frequency and as a result, the data on power factor, efficiency and so on, is very limited. Also, even though it has been suggested that an increased operating frequency may improve system efficiency [10], no data confirming and/or quantifying this is available. Therefore, the power requirement has been assumed to be independent of operating frequency. With a constant power requirement and a varying load resistance, the current requirement will be as shown in Figure 25.

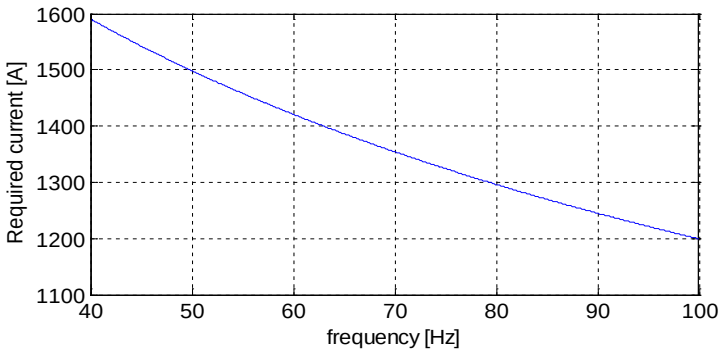

Figure 25: Current required to deliver constant power of P=4 MW

If the assumption of increased efficiency at higher frequencies is correct, the current requirement will be reduced even further. This may reduce the required cross-sectional area of the DEH-cables, and contribute to lower investment costs in addition to the reduced operating costs.

5.2.2 Converter operating power factor

The capacitive compensating unit may be dimensioned so that the converter sees a unity power factor, the load power factor or any power factor in between. It has been suggested that it may be advantageous to operate the MMC at a power factor below unity [36]. To investigate this, simulations have been performed with different compensating capacitance, thereby varying the power factor as seen from the converter. As the converter power factor is reduced, the DC-link

and submodule voltages must be increased accordingly. A summary of the results is shown in Table 8.

Table 8: Converter performance at varying power factor, f=75 Hz

Power factor	1	0.9	0.8	0.7	0.6
SM voltage ripple	30.8 %	29.2 %	28.1 %	25.5 %	22.6 %
THD_i grid	1.8 %	1.8 %	1.9 %	2.1 %	2.2 %
THD_v load	2.3 %	2.5 %	2.7 %	3.1 %	3.6 %

The total harmonic distortion (THD) in the current drawn from the grid, as well as in the load voltage, increases when the power factor seen from the converter is reduced. The THD in the load voltage is not expected to be the most critical factor, but it is important to achieve low THD in the current drawn from the grid, in order to comply with relevant standards. Limits on current harmonics are discussed in section 5.5.

At lower power factors, the percentual voltage ripple in the submodule capacitors is seen to decrease, but this is mainly due to increased average voltage; the absolute ripple is essentially constant. The submodule capacitors work as DC voltage sources, ideally having a constant voltage. In practice they will have a ripple due to charge- and discharge, as described in Table 3. For the DEH application, it seems that the ripple in the capacitors is not critical for acceptable performance. In addition to a reduced overall performance of the converter, operation at a lower power factor will increase system dimensions, thus affecting both weight, volume and cost in a negative manner. The output voltage of the converter is proportional to the inverse of the power factor, and the DC-link voltage and rectifier must be upscaled accordingly. Each submodule must handle a higher voltage, using IGBTs with higher voltage ratings. Perhaps most importantly, lower power factor causes a significant increase in capacitive energy storage required in the system. This outweighs the reduction in compensating capacitors, as shown in Figure 26.

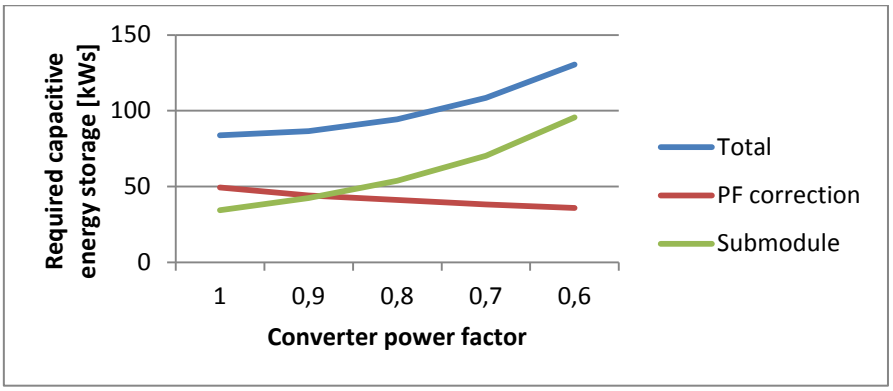

Figure 26: Required capacitive energy storage

For comparison purposes, energy storage capacity is a more convenient unit than capacitance and voltage. Therefore, the values in Figure 26 have been converted according to

$$E_c = \frac{1}{2}CV^2 \tag{5.3}$$

Based on the simulations and the discussion, it seems clear that the load should be fully compensated, thus ensuring that the converter sees a power factor close to unity.

5.2.3 Load data at increased frequency

As a higher operating frequency is one of the key features a converter solution can offer in a DEH system, the simulations and dimensioning have been performed assuming an output frequency of 75 Hz. The choice of frequency is somewhat arbitrary, but is chosen as it is significantly higher than 50 Hz, yet at the same time it is within a realistic frequency range for these purposes. Operating at higher frequencies may also be desirable, but is not investigated further in the thesis.

Many system parameters are frequency dependent, and an overview of key parameters at 75 Hz is found in Table 9.

Table 9: Load parameters at f=75 Hz

Parameter	Value	Unit
Required load current	1324	[A]
Power factor	0.216	inductive
Load resistance	2.28	[Ω]
Load inductance[1]	21.9	[mF]
Apparent power requirement	18.6	[MVA]
Load voltage	14.1	[kV]

[1]Assumed to be constant

5.3 Converter dimensioning

Based on the load data, the converter can be dimensioned. In order to promote modularity, the system should as far as possible be made from standard components.

5.3.1 Converter submodule voltages

From the power factor and required load voltage in Table 9, a required converter output voltage of 3.05 kV is obtained, assuming the series compensating unit supplies all the reactive power. Submodules rated at 690 V_{ac} are chosen as the basic building block for the converter. Having 5 submodules pr. leg arm, one can then produce a maximum voltage of 3.45 kV, thus fulfilling the voltage requirement. By increasing the number of modules from 5 to 6, one adds redundancy by still being able to operate the converter at full voltage and power even in the event of a faulty submodule, as this can then be bypassed. If only 5 submodules pr. arm are active, each of them must handle a higher voltage, as both the DC-link voltage and the output voltage should maintain their pre-fault values.

Table 10: Voltage levels with different number of submodules

Modules pr. arm	6	5	Unit
Max. Output voltage	3.45	3.45	kV
Voltage pr. module (AC)	0.58	0.69	kV
SM-capacitor voltage (DC)	0.81	0.98	kV

Table 10 summarizes the voltage levels within the converter. It is seen that the submodules will operate below their rated voltage when all submodules are healthy, while the voltage levels in the submodules increase to rated level in the event of a disconnection of a faulty submodule.

If a controlled rectifier is used, it would be possible to reduce the DC-link voltage if a submodule required disconnection. One could then avoid overdimensioning the voltage rating of each submodule, but at the expense of a reduced voltage output if a submodule required disconnection. This would not affect a system operating continuously below peak power, but would increase the melting time of hydrates that have already formed.

The maximum obtainable output voltage is slightly higher than the required level. This is desirable, as it gives some margin in case the load power factor is not fully corrected by the compensating unit. It also allows for some variations in output frequency from the design value, which is advantageous if a filter is installed on the DC-link. Instead of tuning the parameters of the filter, the output frequency can be altered to meet the filter resonance frequency. This is discussed further in section 5.4.4.

5.3.2 Submodule capacitor dimensioning

As discussed in 3.3, the submodules ideally operate as ideal voltage sources producing a voltage of either 0 or V_{SM}. However, the voltage across the submodule capacitor will vary when current in either direction flows through it. The relationship between voltage and current for a capacitor is described as

$$i = C\frac{dV}{dt} \tag{5.4}$$

which can be rewritten as

$$dV = \frac{1}{C}\int i\,dt \tag{5.5}$$

From equation (5.5) it is seen that the voltage ripple in the capacitor is inversely proportional to the capacitance for a given current. Hence, the submodule capacitors must be dimensioned sufficiently large to keep the voltage ripple in the capacitors at an acceptable level. Evaluation of equation (5.5) gives

$$\Delta V \propto \frac{1}{C}\int_0^{\pi} i\sin(\omega t)\, d(\omega t) = \frac{2\hat{I}}{\omega C} \tag{5.6}$$

and shows that the voltage ripple also is inversely proportional to the output frequency. However, the voltage ripple cannot be calculated precisely using equation (5.6), as the converter switching causes the current through each capacitor to vary over different time intervals.

In 5.2.1 it was shown that the current requirement was reduced at higher frequencies, which will contribute further to a reduced voltage ripple. Consequently, operation at higher frequencies is advantageous in terms of reduction of the submodule capacitances. As Figure 26 shows, the capacitive energy storage in the submodules are of significant size, and high operating frequency can reduce the weight and volume of these.

Operation with 5 submodules in an arm will cause both the mean value and the peak value of the capacitor voltage to increase and will be the dimensioning scenario in terms of voltage. According to Table 10, the mean voltage of each module will be 980 V with 5 modules in operation. Selecting submodule capacitors rated for 1300V DC will account for the voltage ripple and still maintain a certain safety margin.

When dimensioning the submodule capacitors, the design criterion is that the capacitance must be sufficiently large in order not to influence the converter output significantly, and at the same time ensure the grid influence is within tolerance limits. Through simulations, a capacitor value of 6 mF has been obtained as a minimum value ensuring proper operation of the converter.

The submodule capacitors must be able to handle the current flowing through them. The current through the capacitor will be significantly smaller than the leg arm current, as the current only flows through the capacitor when the submodule outputs a voltage $+V_{SM}$. This can be seen by inspecting Figure 11. When the capacitance is reduced, the maximum allowable current through the capacitor is also reduced, as the number of paralleled units decrease. A possible capacitor to use in the submodules is given below:

- Ducati DC 85 C series, 1 mF, 1300 V_{DC}, I_{rms}= 100 A, 3.5 kg [43]

Using this capacitor would require paralleling of 6 units in each submodule. This would give a maximum current of 600 A through the capacitor. Through simulations, the submodule rms-current has been found to be in the range 400-450 A. The expected lifetime of capacitors is very dependent on operating temperature [43], and having a certain margin to the rated current is advantageous.

With a total of 24 submodules, 144 capacitors will be required, adding 504 kg to the total weight.

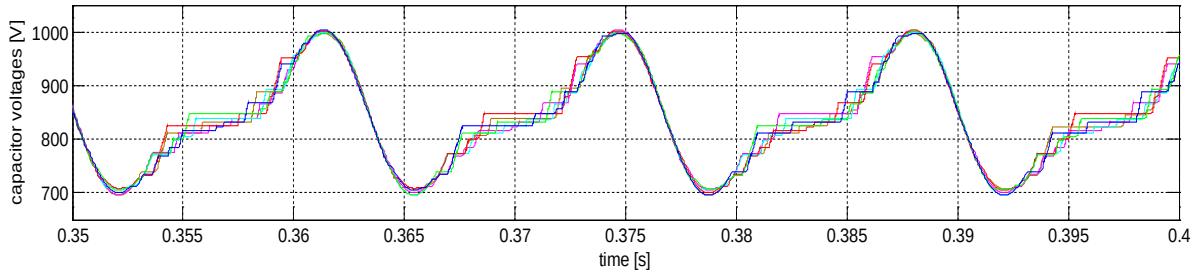

Figure 27: Submodule capacitor voltages, C_{SM}=6 mF

Figure 27 shows the submodule voltages of one leg arm when the submodule capacitance is set to 6 mF. The capacitor voltages are kept within a narrow band with respect to each other by the capacitor balancing algorithms implemented. The voltage ripple is large, but it does not have significant negative influence on either grid or output voltage, and the capacitors are dimensioned to handle the current. The capacitor ripple could be reduced by either increasing the submodule capacitance or by increasing the arm inductance, but both these measures would add to the weight of the system. It could also be possible to implement different PWM-algorithms that are designed to reduce the circulating current, and hence also the voltage ripple in MMC converters [39]. This is beyond the scope of this thesis, and has not been investigated further. A discussion on filters that may reduce the circulating current follows in section 5.4.

Simulations have showed that the converter is able to operate well even with a submodule capacitance below the chosen 6 mF. However, reducing the capacitance will increase the ripple further, and the peak voltage may become too high compared to the design voltage of the capacitors, especially if the arm is operated with only 5 submodules. This is therefore not investigated further.

5.3.3 Submodule switches

As indicated in Figure 11, the MMC submodules include two IGBTs with antiparallel diodes. The IGBTs must be able to block the capacitor voltage V_{SM}, and they must also be able to handle the large current associated with the DEH-application. Due to the MMC structure, the load current is split between the upper and the lower arm [44]. This is also confirmed by simulations, shown in Figure 28. The load current is at its rated value of 1324 A, while the load current is around 800 A. The current in a submodule is shared between its two switches. The load sharing is not even, but still contributes to a lower stress on each module.

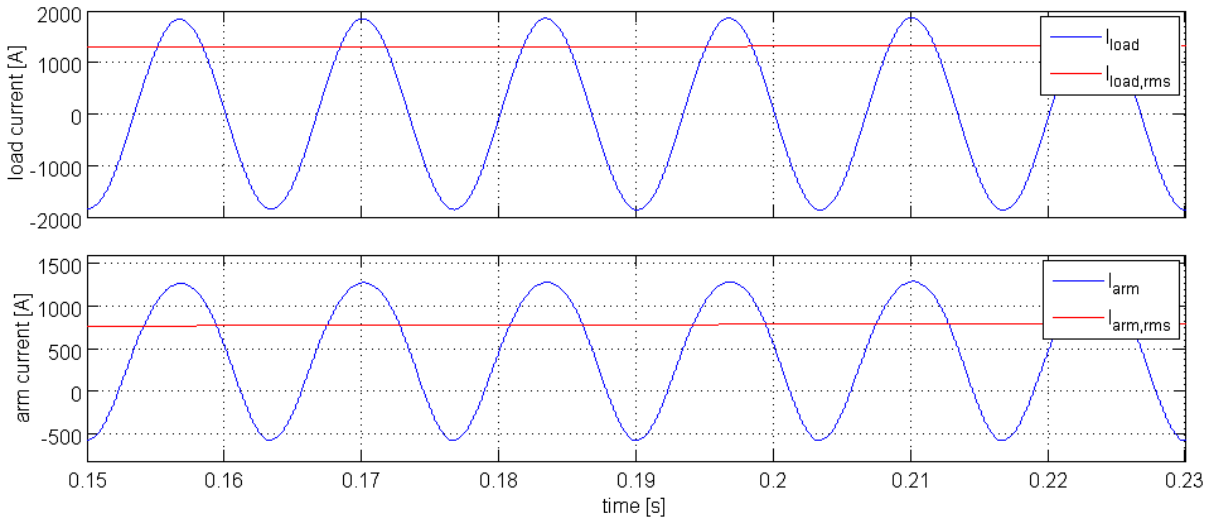

Figure 28: Load current and inverter arm current

Inspecting the figure, it is seen that the arm current contains a significant 2nd harmonic component. This is due to the circulating currents in the converter and is discussed further in section 5.3.5.

The following IGBT modules, rated at 1700 V and 3600 A, are suggested for a SC-HB converter for a similar application [10]:

- Infineon FZ3600R1700HP4_B2 [30]

IGBTs in the same series, rated at currents of 2400 A and 1800 A, are also available [30]. Key parameters for the different IGBTs are found in Table 11. Values are obtained at T_{vj}=125°C and for V_{SM}=900V.

Table 11: IGBT parameters

Rated current	**3600**	**2400**	**1800**	**[A]**
IGBT				
Rated voltage, V_{ces}	1700	1700	1700	[V]
Saturation voltage, $V_{ce,sat}$	2.3	2.3	2.3	[V]
Switching loss (on+off) at rated current	2430	1320	1130	[mJ]
Diode				
Forward voltage	1.65	1.65	1.9	[V]
Reverse recovery energy	1050	840	470	[mJ]

The switching losses are proportional to the current [40], while the losses in the datasheets are referring to different current levels, and they should therefore not be compared directly. Consequently, the 2400 A IGBT will have the lowest switching losses for a given current. Also, the reverse diode associated with the 2400 A and 3600 A IGBTs has a lower voltage drop, thus

giving lower conducting losses than the smallest module. The reverse recovery losses of the diode in the smallest module is however significantly smaller than for the other modules.

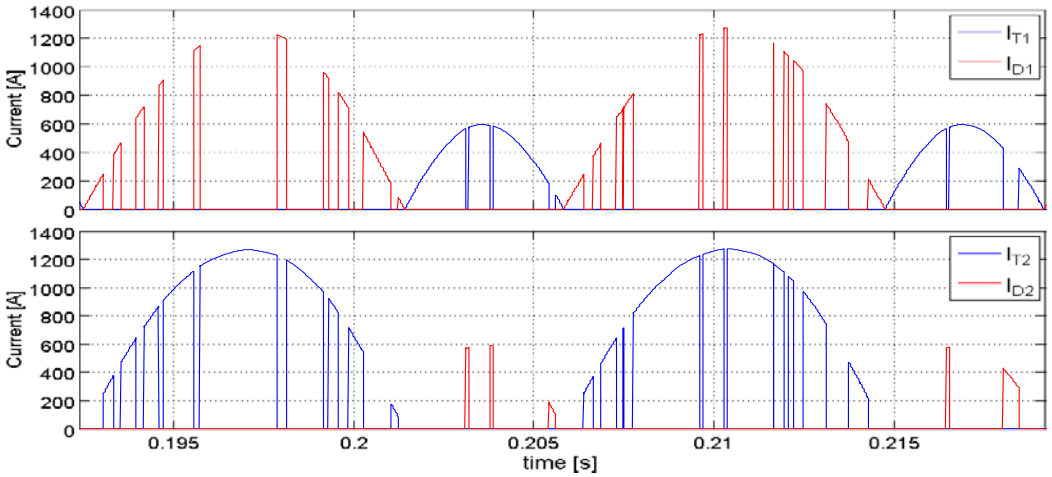

Figure 29: Semiconductor current loading

Figure 29 shows the current through the different semiconductors in a converter submodule. The different semiconductors are very unevenly loaded, with the IGBT T2, as defined in Figure 11 handling the largest share of the current. The uneven loading is a consequence of the DC-offset in the arm current and the zero average current through the submodule capacitor. This may favor IGBTs with higher current ratings than if the loading was more even, which is the case in converters operating at lower power factor, due to their reduced DC-offset. Emphasis should also be placed on IGBTs with a low saturation voltage V_{ces}, with the voltage drop across the diodes being less important due to less prominent conduction losses here.

Both the 2400 A and the 1800 A IGBT are suitable candidates for converter switches. The choice will depend on how robust the converter is designed and the rating of the DEH system. As pointed out in section 3.3, the number of switches required in the MMC will be twice as high as for a SC-HB.

5.3.4 Compensating unit

As discussed in section 2.1, the DEH load has a very inductive nature with a poor power factor. The capacitor compensating unit required to balance this will be a major part in the system. The dimensioning of the compensating unit will be dependent on the operating frequency of the converter.

With the frequency - load power factor relation established and a converter designed to operate around unity power factor, it is possible to determine design parameters for the compensating unit. It can be shown that for a series RLC-circuit, the resonance frequency giving a unity power factor is

$$\omega = \frac{1}{\sqrt{LC}} \tag{5.7}$$

Hence, the required capacitance and voltage of the compensating unit can be obtained as

$$C = \frac{1}{\omega^2 L} = \frac{1}{(2\pi 75)^2 \cdot 21.9 \cdot 10^{-3}} = 205.6\ \mu F \tag{5.8}$$

$$V_{c,rms} = I_{load} Z_c = \frac{I_{load}}{\omega C} = \frac{1324}{2\pi 75 \cdot 205.6 \cdot 10^{-6}} = 13.67\ kV \tag{5.9}$$

In [10], it is suggested using the following capacitor for power factor correction in a DEH system:

- Circutor CHV-M 600/15.2 [45]

This capacitor is rated for 15.2 kV and 600kVAr, corresponding to 8.27 µF. The rated voltage of this capacitor is about 10 % higher than the calculated voltage in equation (5.9), thus allowing for some safety margin. A total of 25 paralleled capacitors are then required to obtain the required capacitance, with each capacitor having dimensions 350x1260x175 mm (WxHxD) and a weight of 81 kg.

5.3.5 Circulating currents and arm inductance

Modular multilevel converters have currents circulating internally in the converter, therefore termed circulating currents. The delivered power to the load oscillates at twice the output frequency, and analogous to this, the energy stored in the capacitors of each leg also oscillates at this frequency [44].

This can also be observed by noting that the energy stored in a capacitor is proportional to the capacitor voltage squared. Figure 30 shows the capacitor voltages in the upper and lower arm of a leg and the resulting stored energy in the leg. The relative stored energy in the leg is obtained by adding the square of the capacitor voltages in the upper and lower arm and is proportional to the stored energy. As the energy in the legs varies, current flows back and forth between the legs to even out the energy unbalance between them.

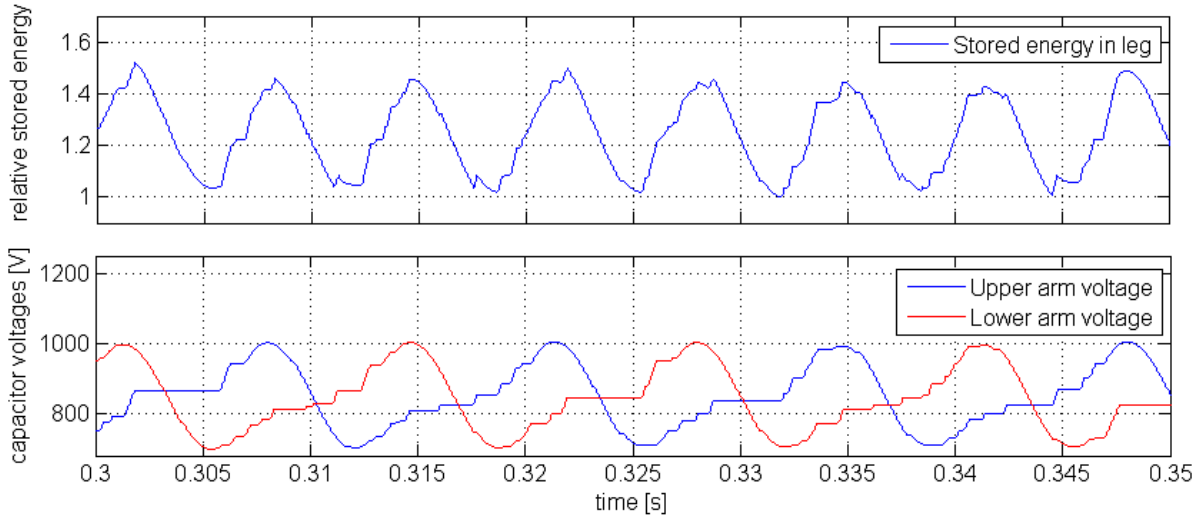

Figure 30: Stored energy in leg capacitors (top), capacitor voltages (bottom).

The arm current can be described as [46]:

$$i_{arm}(t) = \frac{I_d}{2} \pm \frac{i_{line}(t)}{2} + i_{circ}(t) \tag{5.10}$$

Where

- I_d = Current flowing in the DC-link.
- i_{line} = Current in the line connected to the converter arm, equal to the load current in a single-phase converter. The sign is opposite for the upper and lower arms.
- i_{circ} = Circulating current flowing internally in the converter.

Equation (5.10) was given for three-phase converters, where a third of the DC-link current would flow in each arm, but the DC-term has been adjusted to fit with the two legs associated with a single-phase converter. The sign of the line term is opposite for the upper and lower leg arm.

Further, the circulating current in equation (5.10) can be expressed as [44]:

$$i_{circ}(t) = \frac{U_{2f}}{4\omega_0 L_{arm}} \cos(2\omega_0 t + \varphi) \tag{5.11}$$

Where

- U_{2f} = Amplitude of the double-fundamental-frequency equivalent voltages
- L_{arm} = Inductance in leg arm

Equation (5.11) shows that the circulating current can be reduced by increasing the arm inductance. The circulating current causes higher losses in the converter and also increases the voltage ripple in the submodule capacitors by increasing the current flowing through them.

In Table 12, the results from a Fourier-analysis of the arm current are given, showing the different components in equation (5.10).

Table 12: Harmonic content in arm current

Harmonic	Amplitude [A]
DC	444
1st	935
2nd	70

The DC-component has been compared to the current in the DC-link, and is confirmed to be 50 % of this. According to equation (5.10), the fundamental component should equal 50 % of the load current. This is confirmed by doubling the fundamental component and dividing it by the square root of two to obtain the rms-value. This yields 1322 A, close to the required load current of 1324 A given in Table 9.

The 2nd harmonic is 7.5 % of the fundamental. As equation (5.11) shows, the circulating current is inversely proportional to the arm inductance. A larger arm inductance would therefore contribute to lower losses in the converter. However, the physical dimensions of the arm inductor become large for applications involving large currents, as is the case in DEH application. The physical dimensions of an inductor can be approximated to those of a transformer with the following rating [25]:

$$S = p \cdot \omega \cdot L \cdot \frac{\hat{I}}{\sqrt{2}} \cdot \frac{I_{rms}}{2} \tag{5.12}$$

Where

- S = rated power (VA)
- p = number of phases (single or three)
- ω = angular frequency
- $\hat{I}$ = The peak current observed in inductor
- I_{rms} = rms current in inductor

In the simulations an arm inductance of 1.5 mH is used. A typical value of the arm inductance is 1-1.2 mH [47], hence the selected parameter represents a relatively high value. Inserting 1.5 mH and the arm current shown in Figure 28, a transformer rated power of 240 kVA is obtained. This gives an inductor weight of approximately 700 kg pr. arm, totaling 2800 kg for the 4 leg arms. Details on weight estimation are given in Appendix C. In section 5.4.2, it is discussed how the size of the arm inductor may be reduced, given an appropriately designed filter is installed on the DC-link.

In addition to limiting currents flowing in the converter, the arm reactor also serves a purpose in limiting the current rise rate during fault conditions [44]. Assuming a constant voltage in the submodules during a DC-link short circuit and equal current rise rate in the two leg arms, Kirchhoff's Voltage Law yields [44]:

$$2L_{arm}\frac{di}{dt} - U_{dc} = 0 \tag{5.13}$$

Introducing

$$\alpha = \frac{di}{dt} = \frac{U_{dc}}{2L_{arm}} \tag{5.14}$$

a design principle for the arm inductance can be expressed in terms of the fault current rise rate, α.

$$L_{arm} = \frac{U_{dc}}{2\alpha} \tag{5.15}$$

It is therefore also possible to dimension the arm inductor to keep the current rise rate below a certain value.

5.4 Filter on DC-link

The DEH-load is a large single-phase system, and the power delivered to the compensated load can be expressed as:

$$P_{load}(t) = \hat{V}\sin(\omega t)\cdot\hat{I}\sin(\omega t) = \hat{V}\hat{I}\cdot(1-\cos\ (2\omega t)) \tag{5.16}$$

As opposed to a balanced three-phase system usually associated with large loads , the single-phase DEH-load power will pulsate with twice the output frequency, as equation (5.16) shows. These pulsations are partially handled by the capacitive energy storage in the submodules, but very large submodule capacitances are required in order to achieve a constant power factor drawn from the grid. Therefore, the power pulsations on the grid must be handled by other means.

Two different passive filter configurations have been investigated as alternatives for eliminating 2nd harmonic oscillations on the grid, these are illustrated in Figure 31.

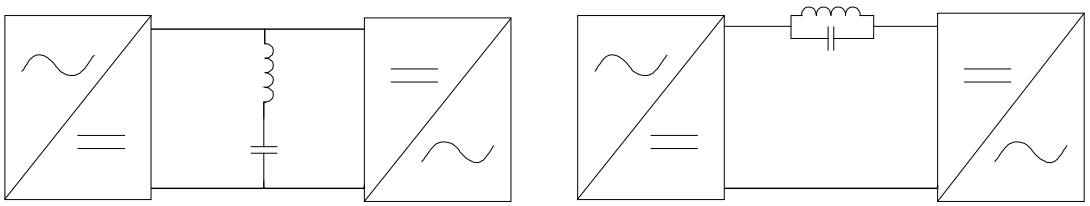

Figure 31: Resonant band-pass filter (left), resonant band-stop filter (right)

5.4.1 Band-pass filter

A possible solution is to install a band-pass filter on the DC-bus. If properly tuned, such a filter can eliminate pulsations at a given frequency. The strategy of the band-pass filter is to let the filter supply the 2nd harmonic current required by the load, thereby drawing a constant power from the grid.

Assuming a negligible resistance, the impedance of a series LC-circuit can be expressed as

$$Z = j\omega L - \frac{j}{\omega C} \tag{5.17}$$

At a given frequency, termed the resonance frequency, the impedance of such a circuit will approach zero [48]. The resonance frequency of a given circuit is obtained by equating equation (5.17) to 0, yielding

$$\omega_c = \frac{1}{\sqrt{LC}} \tag{5.18}$$

For an output frequency of 75 Hz, the relationship between L and C filtering the 150 Hz harmonics is then expressed as

$$L = \frac{1}{(4\pi 75)^2 C} \tag{5.19}$$

Different values of L and C will cause different behavior of the filter. Figure 32 shows the frequency-impedance relation for different values of C, with L being calculated from the equation above. The filter must be fine-tuned to give the desired performance. Reducing the capacitance and thus increasing the inductance correspondingly, will give reduced frequency sensitivity. This means the resonance frequency will be the same but with low impedance also at frequencies near the resonance frequency, thus making the tuning of the filter less critical. The figure also illustrates that a deviation in either L or C will give a different resonance frequency. In the figure, the capacitance C_4 is 10 % too high, which causes the resonance frequency to be reduced almost 5 % and gives a higher impedance at the intended frequency. This resonance frequency reduction is in accordance with equation (5.18).

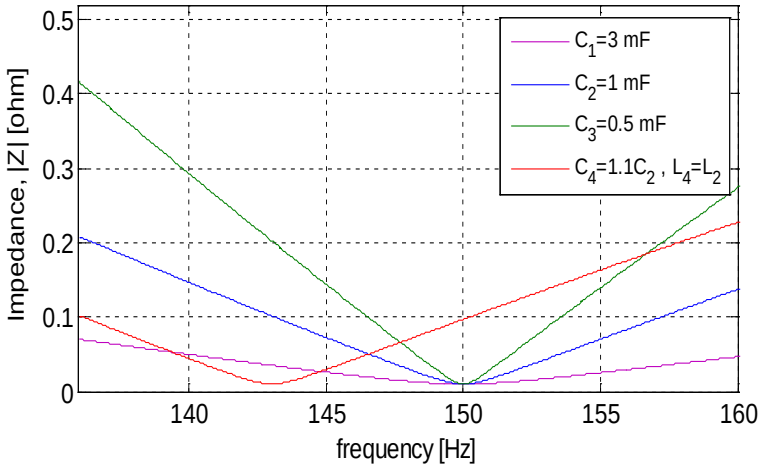

Figure 32: LC-filter impedance vs. frequency

Figure 33 shows the instantaneous power drawn from the grid, a capacitance of 1 mF has been used in the simulations. The band-pass filter illustrated in Figure 31 is applied at t = 0.3 s. Without a filter, the power oscillations are almost 1.5 MW peak-to-peak. It is evident that when the filter is activated, the large 2nd harmonic oscillations on the grid are efficiently eliminated, and the instantaneous power becomes essentially constant after some settling time. The THD in the current drawn from the grid is 2% after activation of the filter, with the 17th and 19th harmonic being most prominent, along with some 2nd and 3rd harmonic.

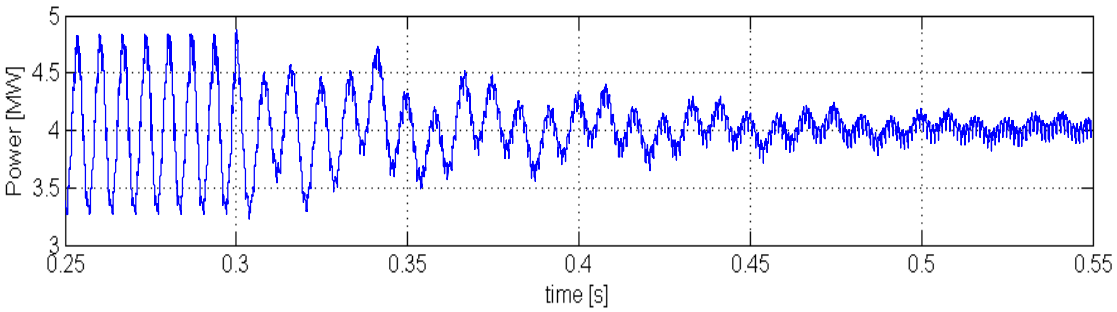

Figure 33: Instantaneous power drawn from the grid, filter applied at t = 0.3s

Although the band-pass filter is efficient in assuring constant power drawn from the grid, it has a negative effect on other parts of the system. As discussed above, the 2nd harmonic component of the arm current is due to the oscillations in stored capacitor energy at this frequency. Having a filter giving very small impedance at this frequency thus increases the arm currents. Figure 34 shows how the 2nd harmonic current is increased when the filter is activated.

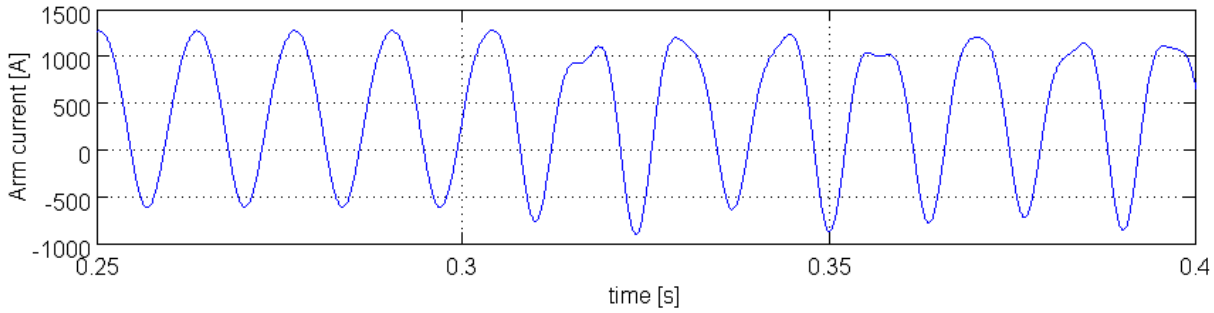

Figure 34: Arm current, band-pass filter activated at t = 0.3 s

This additional current is not a circulating current flowing between the two inverter legs, but current flowing between the individual legs and the filter on the DC-link. The effect however, will be the same as for the circulating currents; it will not affect the grid or output, but it will increase converter losses and increase the voltage ripple in the submodule capacitors. When the filter is activated, the arm rms-current increases from 780 to 795 A, and the rms-current through the submodule capacitors increases from 400 to 450 A, thus increasing the capacitor voltage ripple. The voltages and current in the filter are given in Figure 35.

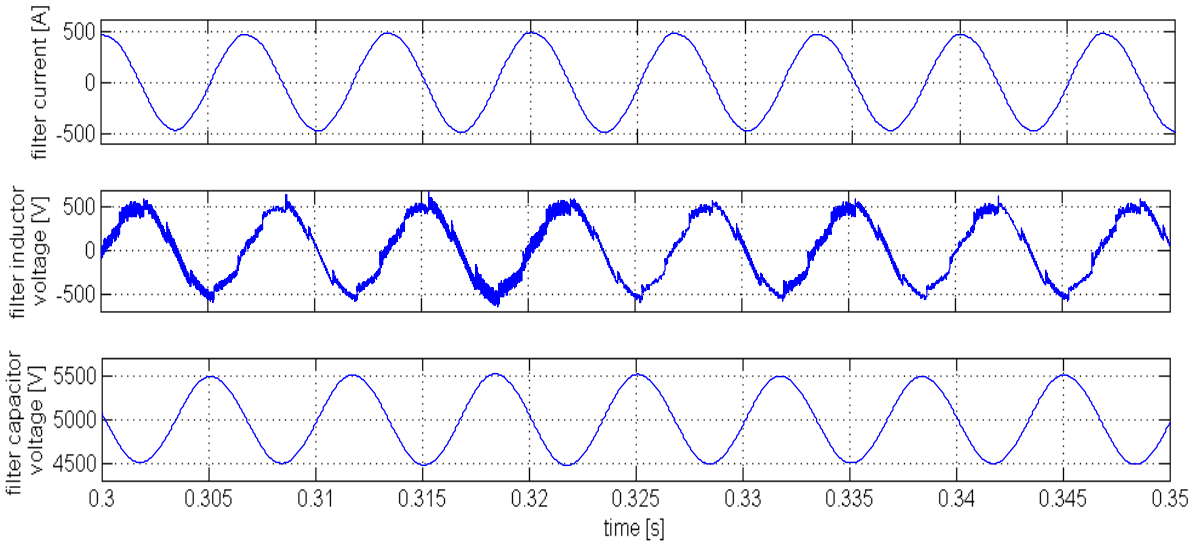

Figure 35: Band-pass filter current and voltages

5.4.2 Band-stop filter

As an alternative to the band-pass filter, simulations have been performed on a band-stop filter, as illustrated in Figure 31. The strategy of the band-stop filter is to give high impedance between the grid and the inverter at a frequency matching the 2nd harmonic and therefore draw a constant power from the grid. The time-varying output power must then be taken care of by the capacitive energy storage in the submodules. The resonance frequency and the relationship between the inductive and capacitive parts of the filter is the same as for the band-pass filter, as described in equation (5.18) and (5.19). The impedance for an ideal band-pass filter when neglecting resistance is:

$$Z = \frac{j\omega L}{1 - \omega^2 LC} \tag{5.20}$$

As opposed to the band-pass filter discussed in the previous section, having a large capacitance in the filter will give reduced frequency sensitivity. When including a finite resistance in the filter branches, the peak impedance at resonance frequency will not approach infinity, as equation (5.20) suggests, but instead it will have a finite peak depending on the filter parameters. Both a large resistance and a large capacitance will reduce the maximum impedance. Smaller capacitances will thus give a narrower peak with increased peak impedance magnitude at resonance frequency.

The performance of the converter has been evaluated for different filter parameters, and the results are summarized in Table 13. A 20 mΩ resistance has been included in both the inductive and capacitive the branch throughout the simulations.

Table 13: Inverter performance with different filter parameters

Capacitance [mF]	No filter	3.0	1.0	0.5	0.1	Unit
Inductance	-	0.375	1.13	2.25	11.3	mH
V_{thd} grid	2.3	1.9	1.5	1.5	1.6	%
I_{thd} grid	17.8	7.4	1.8	1.7	1.9	%
I_{arm} 2nd harm.	8.1	5.6	0.9	0.4	0.2	%
$V_{sm,\ ripple}$ pk-pk	270	263	252	250	250	V
DC-link voltage ripple	6.6	8.7	9.9	9.9	9.9	%
SM-cap. current	395	380	370	370	370	A
Filter current ripple	-	1840	900	450	120	A
$V_{filter,rms}$	-	232	336	354	495	V
Equivalent transformer rating		102	228	380	1620	kVA
Estimated inductor weight		400	700	1000	3000	kg
Capacitor weight		12	8	4	2	kg
Total filter weight		412	708	1004	3002	kg

The equivalent transformer rating is calculated from (5.12) and is used for weight estimation of the inductor. The table points out the general trend, which is that the performance of the inverter is increasing as the filter capacitance is reduced. The largest capacitance value, 3 mF, is seen to only have minor performance improvement compared to the reference case where no filter is applied. The most important parameter in the table, is the THD of the current drawn from the grid. This value is unacceptably high for large filter capacitances but remains essentially constant at a low value for smaller filter capacitances. For an appropriate filter dimensioning, it is therefore possible to achieve the target of minimizing the 2nd harmonic component in the power drawn from the grid. This will also have a positive influence on the THD of the grid voltage, but this value is small also without the use of a filter and is as such not a dimensioning criterion. As the

power drawn from the grid is essentially constant, the capacitive storage in the submodules must handle the time-varying power drawn from the load. The table shows that they are capable of doing so, and in addition, the voltage ripple is reduced due to the small 2nd harmonic current.

A very interesting observation is that the 2nd harmonic component of the arm current, the circulating current, can essentially be eliminated for small values of filter capacitance. This is a large contrast to the band-pass filter, which greatly increased the 2nd harmonic component of the arm current. Eliminating the circulating current reduces inverter losses, and it is also the reason the ripple in the submodule capacitor voltage is somewhat reduced.

A closer inspection of the inverter reveals the reason why the circulating current of the single-phase MMC can be eliminated using a resonant band-stop filter. The filter ideally blocks all 2nd harmonic current fluctuating between the grid and the inverter, consequently the only contribution to this current must be a component flowing between the two inverter legs. The phenomenon of circulating currents was discussed in section 5.3.4, and it was argued that the circulating current is caused by an unbalance in the stored energy in the submodule capacitors of the different legs. In Figure 30 the submodule capacitor voltages and the corresponding capacitor energy was shown, and the figure is for the reader's convenience repeated below.

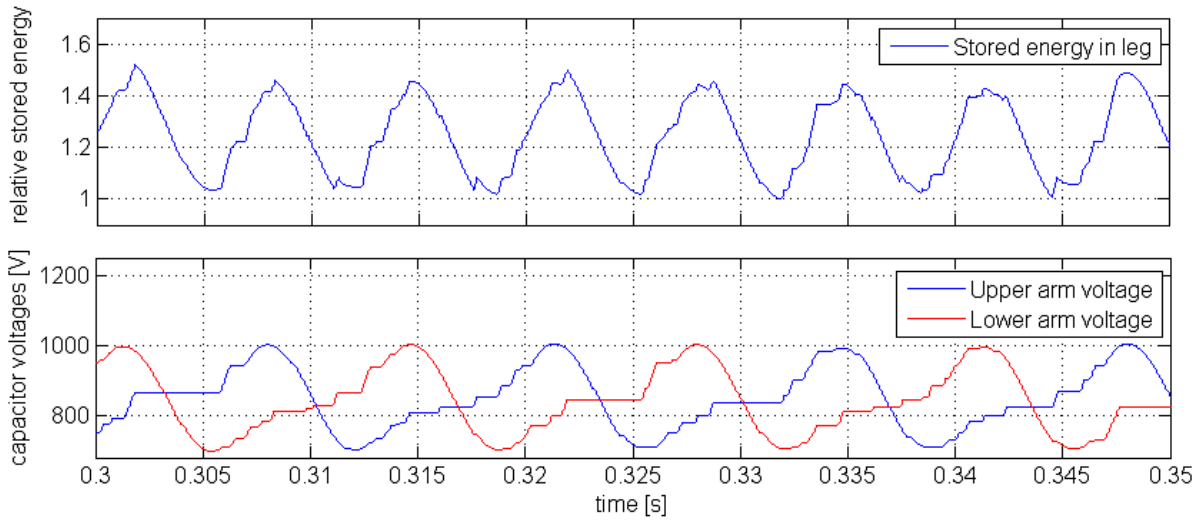

Figure 36: Stored energy in leg capacitors (top), capacitor voltages (bottom).

Only one submodule capacitor voltage pr. arm is given in Figure 36, but the voltages of the different submodules have previously been shown to vary within a narrow band. This simplification makes the figure more intuitive without introducing an error in the discussion that follows.

The figure shows that the capacitor voltages of the upper and lower arm in a leg are 180° out of phase, an observation supported by the ± term in equation (5.10). This causes the variation in total stored energy in the leg as is also indicated in the figure. In a three-phase MMC, the line

currents will be shifted 120° with respect to each other, thus causing the capacitor voltages and the stored energy to be shifted with the same amount. In a single-phase MMC, the two converter legs are shifted 180° apart, causing the upper arm capacitor voltages of one leg to be in phase with the lower arm capacitor voltages of the other leg. The stored energy oscillations in the two legs are therefore in phase and thus keeps the current flowing between the legs at a marginal level.

From this, it is possible to conclude that the 2nd harmonic component in the arm current of single-phase MMCs is not a circulating current in the same way as found in three-phase converters but a component caused by the time-varying instantaneous output power as seen from the DC-link. By introducing a band-stop filter blocking these oscillations in the power drawn from the grid, the 2nd harmonic current in the converter legs is removed as a bonus. This has positive implications beyond the improved converter performance shown in Table 13. With the 2nd harmonic current component already removed, the circulating current suppression is no longer as important as a dimensioning criterion for the arm inductor, and this creates a potential for reduction of this parameter. The arm inductor is a heavy component, and this may lead to a significant weight reduction. Simulations have shown that an arm inductance as small as 0.7 mH is sufficient to keep the 2nd harmonic in the arm current at 1.0 % of the fundamental with the band-stop filter installed.

It should be pointed out that the arm inductor by no means must be omitted. Even though the stored energy in the leg capacitors are in phase, they will in practice never be perfectly balanced, and some inductance should therefore be present to prevent this from introducing significant circulating currents. As discussed in section 5.3.4, the arm inductor also serves a purpose in limiting the current rise-rate in the event of a short circuit. This is therefore likely to be the dimensioning criterion for the arm inductor.

5.4.3 Selection of filter

Based on the evaluation of the two different filter alternatives, it is clear that the band-stop filter has superior qualities compared to the band-pass filter. They both achieve reducing the THD on the grid significantly, but the band-stop configuration eliminates the 2nd harmonic component in the arm current, whereas the band-pass filter amplifies it significantly. The resonant band-stop filter on the DC-link will therefore be the configuration of choice.

From Table 13 it is clear that the performance of the filter is essentially unchanged if the filter capacitance is reduced beyond 1 mF. The inductor is by far the dominant component in terms of weight, and it should therefore be kept as small as possible without compromising the performance of the filter. A filter with a capacitance of 1 mF and an inductance of 1.13 mH is therefore selected. This will give a calculated filter weight of approximately 700 kg. Details on the weight calculations are found in Appendix C.

Figure 37 shows the impedance of the selected filter.

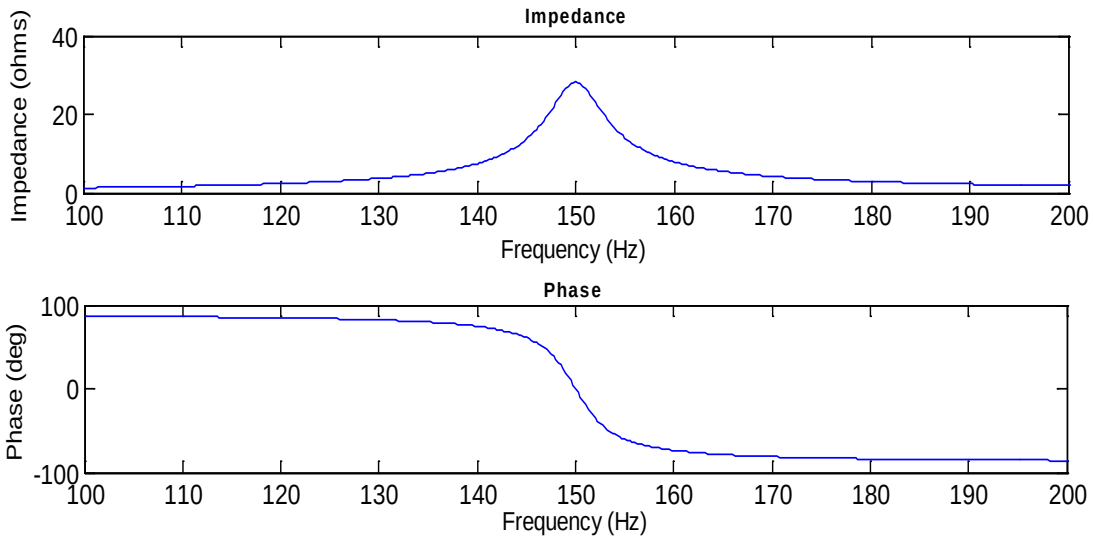

Figure 37: Magnitude and phase plot of filter impedance

The frequency sensitivity of the filter has not been a dimension criterion. High frequency sensitivity requires more precise tuning than a filter with a less steep impedance-frequency curve. Unlike most other applications, there is no strict requirement for the operating frequency of the converter. For small variations around the design frequency, it will therefore be possible to adjust the operating frequency to match the actual resonance frequency of the filter. This will reduce the need for a very precise filter tuning.

5.4.4 Frequency tuning of a resonant filter

It may in practice prove difficult to implement a filter with the exact right parameters to resonate at twice the output frequency, and this will result in the resonance frequency being either higher or lower than the design criterion. Having a poorly tuned filter may result in undesired power pulsations on the mains. If this becomes a problem, a solution could be to adjust the output frequency to half of the actual resonance frequency. If the resonance frequency of the filter is reasonably near the design value, a small change in output frequency will be sufficient to compensate for this. Unlike many typical converter applications such as motor drives, a converter feeding a DEH load does not have a specific criterion dictating the output frequency. No parts of the DEH system are believed to be noticeably affected by a small frequency change. The power factor seen from the converter will only experience small deviations for small frequency variations, and the converter should either way be dimensioned to handle this. Small variations in frequency are also unlikely to cause a large impact on the system efficiency. It would therefore be possible to adapt the output frequency to make the 2nd harmonic match the filter's resonance frequency.

One drawback of adjusting the output frequency to tune the filter is that it reduces the freedom to tune the output frequency to obtain a unity power factor as seen from the converter terminals. The compensating unit may in practice not be properly tuned to the load inductance at the design frequency, due to deviations from assumed values in either capacitance or load inductance. The power factor, PF, seen from the converter, can be expressed as

$$PF = \frac{R}{\sqrt{R^2 + (\omega L - \frac{1}{\omega C})^2}} \tag{5.21}$$

In order to investigate the sensitivity to inaccurate inductance and capacitance, one may assign the value 1 to the load resistance and approximate the reactance to be the inverse of the load power factor, a condition that holds well for low power factors. This yields

$$PF = \frac{1}{\sqrt{1 + \frac{1}{PF_{load}^2} \cdot (\frac{L}{L_0} - \frac{C_0}{C})^2}} \tag{5.22}$$

The result is plotted in Figure 38. It shows that the converter will operate at a high power factor, even in the event of small deviations in inductance or capacitance. The power factor may only become noticeably reduced in the event that a substantially larger inductance is followed by a correspondingly large capacitance or if both are significantly smaller than assumed. In this case, it would be advantageous to be able to adjust the operating frequency to increase the power factor and not be limited by a specific frequency being required due to the filter. On the other hand, if the load inductance and the compensating capacitance have been determined accurately, or their deviations counteract each other, the power factor at design frequency will be close to unity. In such a situation, small frequency variations to tune the DC-filter can be made while maintaining a high power factor.

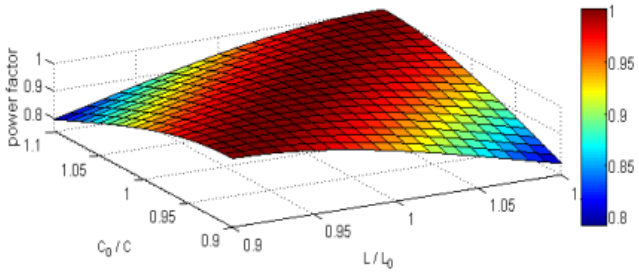

Figure 38: Converter PF for deviations in inductance/capacitance, PF_{load}=0.25

Adjusting the output frequency to tune the filter should thus only be problematic in a worst case scenario where the load inductance and compensating capacitance both deviate significantly, and their combined inaccuracies amplify the error. In addition, the inaccuracy in the DC-filter parameters must then require an output frequency worsening this error further. To avoid this problem, effort should be placed on achieving as high accuracy as possible in the DC-filter parameters. Accurate power factor compensation at a given frequency requires accurate data on the load inductance. In addition, the converter should be dimensioned to handle power factors somewhat below unity.

If one allows for tuning of the filter during commissioning, one can first experimentally determine the output frequency giving unity power factor and dimension the filter parameters after this. The final tuning of the filter can then be performed by frequency variation, as the power factor will be kept high.

5.5 Harmonics and flickers

The use of power electronics introduces harmonics in an electrical system due to the switching actions of the power semiconductors. Standards have been created to regulate the amount of harmonics that is tolerable at the point of common coupling (PCC). If the harmonics at PCC become too large, it may influence other components on the network and filtering may be required.

5.5.1 IEEE standard limits

Although there are various standards suggesting limits for flickers and harmonics, the following standard has been used as a guideline in this thesis:

- IEEE Standard 519 – Recommended Practices and Requirements for Harmonic Control in Electrical Power Systems [49]

The following tables are extracted from the standard, and are used to evaluate the performance of the converter.

Table 14: IEEE Standard 519; Table 11.1 Voltage distortion limits

Voltage distortion limits	
Individual harmonic	3.0 %
THD	5.0 %

Table 15: IEEE Standard 519; Table 10.3 Current distortion limits

Current Distortion Limits	
Harmonic	Amplitude
h < 11	4.0%
11 ≤ h < 17	2.0%
17 ≤ h < 23	1.5%
23 ≤ h < 35	0.6%
35 ≤ h	0.3%
THD	5.0%

Table 15 only lists the requirement for odd harmonics; even harmonics are limited to 25 % of the odd harmonics.

5.5.2 Grid influence without filter

To this point in the thesis, it has been assumed that action must be taken to avoid the time-varying power drawn by the load from influencing the grid, and filters have been designed for this purpose. To justify this assumption, a Fourier analysis of the current drawn from the grid is shown in Figure 39.

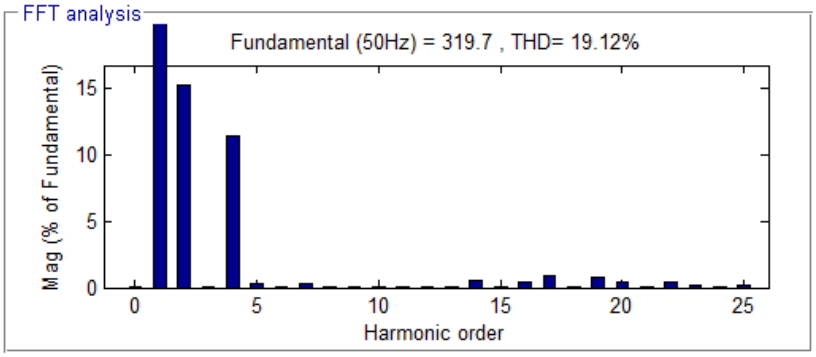

Figure 39: Fourier analysis of current drawn from grid with no filter on DC-link

The figure shows that there are very large 2nd and 4th harmonic components exceeding the limits given in Table 15. The voltage is also unbalanced under these operating conditions, but this is not shown here, as Figure 39 is sufficient to confirm that filtering is needed.

5.5.3 Grid influence with resonant band-stop filter

When the resonant band-stop filter discussed in section 5.4.2 is applied, the current drawn from the grid was shown to be essentially constant. This also implies that the harmonics in the current should be significantly reduced. Figure 40 shows the harmonic spectrum of the input current when the band-stop filter is applied.

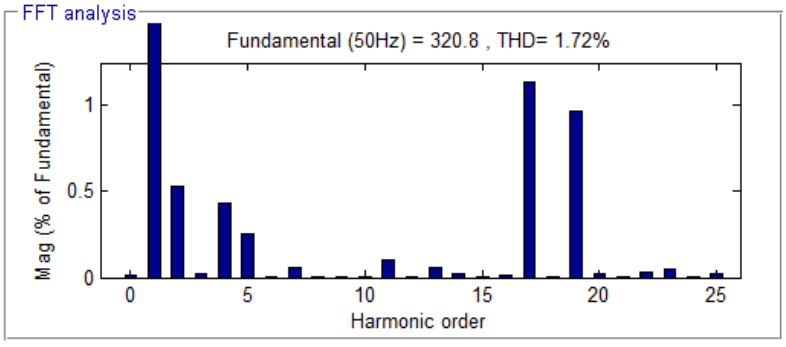

Figure 40: Fourier analysis of current drawn from grid using band-stop filter

The figure shows that the 17th and 19th harmonics are the most prominent, and they are caused by the 18 pulse rectifier. According to Table 15, the limit of these harmonics is 1.5 %, and the figure shows that they both are below this value. The figure also shows that there still are some 2nd and 4th harmonic components present. As the limit of even harmonics is only 25 % of the odd harmonic limits, they must be kept below 1 %, a requirement they fulfill. Due to the strict requirement for even harmonics, and a 2nd harmonic component always present in single-phase

inverters, this component may in practice often be the most difficult to keep within the limits. The THD of 1.7 % is well below the maximum allowance of 5.0 %.

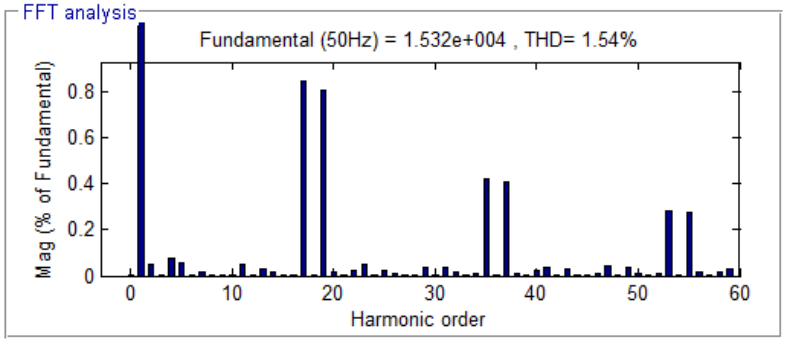

Figure 41: Harmonic spectrum of grid voltage with band-stop filter applied

Figure 41 shows the harmonic spectrum of the grid voltage when a band-stop filter is applied. As expected, the harmonics around the multiples of the pulse number for the rectifier are the most prominent, but both the individual harmonics and the THD are well below the limits stated in Table 14.

This shows that the band-stop filter is capable of ensuring proper operation of the converter without having unacceptable influence on the grid.

5.5.4 Flickers

Flickers are a result of a load varying over time and are causing repeated voltage drops that may influence sensitive electronic equipment or give fluctuation in lights connected to the same grid [49]. The IEEE standard 519 is vague on flickers and does not provide actual limits for voltage flickers. However, it does provide information on the percentual voltage fluctuation tolerated for a given flicker frequency before it becomes a visual problem to humans in terms of lighting.

For frequencies of 3-10 Hz, a voltage fluctuation below 0.5 % is listed as tolerable for humans, while higher fluctuations are tolerated for higher frequencies.

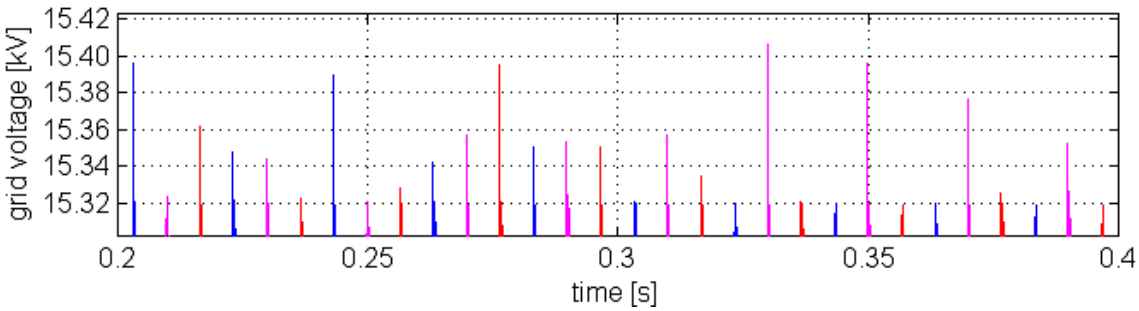

Figure 42: Grid voltage peaks at output frequency of 75 Hz

In Figure 42, the grid voltage is plotted. The view is zoomed in to show the voltage peaks. From the figure it is seen that the voltage peaks all lie within an 80 V band, which corresponds to $\Delta V/V$

= 0.52 %, with a frequency that appears to be random but certainly above 10 Hz. Despite the standard being vague on flicker limits, it could seem reasonable to assume that this is tolerable.

Throughout the thesis, an output frequency of 75 Hz has been used. However, the 2nd harmonic of this frequency is a multiple of the grid frequency of 50 Hz. This might influence the flickers in the grid voltage. To check if other results occur at different frequencies, simulations with an output frequency of 83 Hz has also been performed. The resulting grid voltage is shown in Figure 43.

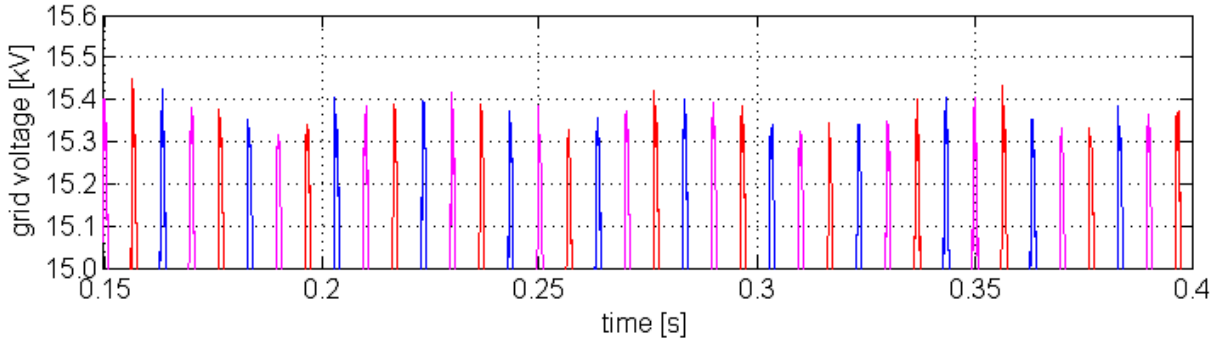

Figure 43: Grid voltage peaks at output frequency of 83 Hz

At this frequency the flickers occur in a more regular manner with a fixed frequency, estimated to 15 Hz. The voltage ripple is approximately 105 V and corresponds to $\Delta V/V$ = 0.68 %. According to the IEEE standard, this is very near the limit where it becomes noticeable to the human eye.

If a power electronics source for DEH application is to be constructed, then the flickers it causes on the grid should be investigated further. The grid used in the simulations is a relatively weak grid, thus making the estimate of converter performance in terms of flickers conservative. If connected to a larger grid, the flickers will become less significant. The operating frequency is also a factor that must be considered when evaluating the flickers, but there is nothing suggesting flickers will be a significant problem if a converter is utilized as a DEH source. There are also several measures that can be taken if flickers should become a problem [49]. Other standards have quantified limits for flickers, and there are apparatus available to measure and quantify flickers [50]. However, this has not been investigated further.

5.5.5 Other harmonic considerations

As the band-pass filter was shown to have reduced overall performance compared to the band-stop filter, it has not been evaluated in terms of harmonics. However, the power oscillations on the DC-side were greatly reduced by this filter as well, and the band-pass filter is thus assumed to cause similar harmonic content on the grid as the band-stop filter.

The converter output voltage has a THD of 10.5 %, with the prominent harmonics centered around 6000 Hz, which is twice the switching frequency of the converter legs at 75 Hz. The highest individual harmonic is 3.0 %. Due to the large compensating capacitor, the load voltage

only has a THD of 2.3 %, and the load current has a THD of 0.2 %. The inductive load and the compensating unit act as large filters making the load current and load voltage insensitive to the converter output. Therefore, the converter output harmonic content has not played an important role in the dimensioning of the converter. It may also be possible to reduce the switching frequency, in order to reduce converter losses without compromising the load harmonics.

5.6 Switching algorithms

As discussed in section 4.2.2, two different algorithms for submodule capacitor voltage balancing have been implemented. The normal switching algorithm is primarily focused on achieving the best possible voltage balancing, while the reduced switching frequency algorithm is focused on keeping the switching losses low by avoiding excess switching. With the rest of the system dimensioned, it is possible to evaluate the performance of these algorithms. Throughout the dimensioning process, the algorithm giving the best voltage balancing was used.

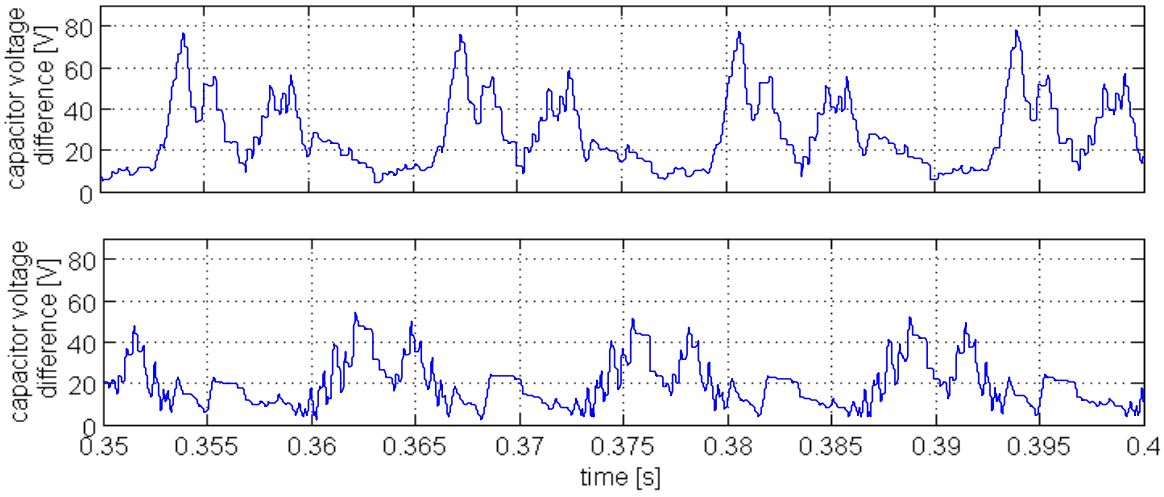

Figure 44: Voltage differences using the RSF (top) and the normal algorithm (bottom)

Figure 44 shows the voltage difference between the most and least charged capacitor in a leg arm when using the two different algorithms. It can be seen that both the peak and the average voltage difference are higher when using the reduced switching frequency (RSF) algorithm. The switching frequencies for each IGBT is found to be 500 Hz and 970 Hz for the RSF and normal algorithms respectively. For the RSF algorithm, the switching frequency is given solely by the PWM-algorithm.

The performance of the converter using the RSF has been evaluated, and there seems to be no noticeable behavior change from simulations using the normal algorithm. The harmonics in the current from the grid, shown to be one of the most critical factors, are equal with a THD of 1.72

%. The ripple in the submodule capacitor voltages are also identical, and the 2nd harmonic internal current is still below 1 % of the fundamental.

As there are no apparent reasons to choose the normal algorithm over the RSF, and due to the switching losses being twice as high using the normal algorithm, the RSF is recommended used in DEH application.

No noticeable reduction of performance on the grid or converter internal is apparent when using an algorithm causing a reduced frequency, and the load is assumed not to be sensitive to harmonics. This suggests that the switching frequency can be reduced even further by reducing the frequency modulation index, without compromising the converter performance. This has not been examined but should be investigated further should a real system be installed.

5.7 Special considerations

There are some aspects that deserve extra highlighting when it comes to designing a power electronic converter for a DEH system.

5.7.1 Common mode voltage

As illustrated in Figure 2, the DEH concept requires one of the converter terminals to be connected to the near end of the grounded pipeline, meaning the converter terminal itself is in practice grounded. Therefore, the converter by design operates with an earth fault. The different parts of the converter will thus operate with a voltage with respect to ground, fluctuating as the converter switching state changes.

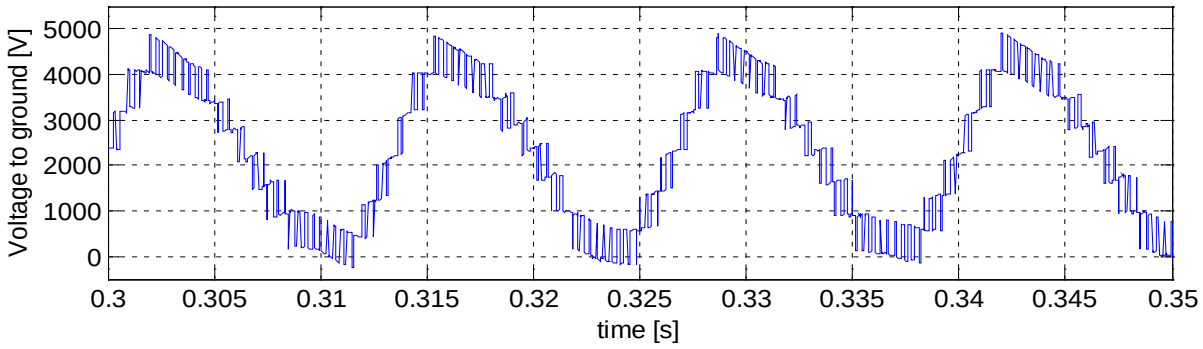

Figure 45: Upper DC-rail voltage to ground

Figure 45 shows how the voltage between the upper DC-rail and ground fluctuates when one of the converter legs is grounded. Other parts of the converter will experience the same fluctuations. Due to this, all converter components must be sufficiently insulated from ground to withstand voltage stress. The DC-link voltage will be the maximum voltage with respect to ground any component will experience. The phase-shifting transformers create galvanic isolation between the grid and the converter and should have an isolated secondary neutral.

The common mode voltage with a magnitude as high as the DC-link voltage will introduce common mode currents through stray capacitances throughout the different parts of the converter. This has not been evaluated further in the thesis but is a topic requiring attention if an actual converter solution for DEH is constructed. Focus should be both on analyzing and reducing the consequences of the common mode voltage. Common mode noise can be a significant source of electromagnetic interference (EMI) [40].

5.7.2 System simplicity

It has already been pointed out that the DEH load is an unusually unsophisticated load to be fed from a power converter. Wherever possible, this is a feature that should be taken advantage of. The control system can have a reduced complexity, as voltage and frequency are held constant throughout operation. The converter must still have appropriate protection systems installed, that can protect both the converter and load should a fault occur.

The voltage ripple in the submodule capacitors are shown to be large. This can be tolerated as the inductive load and the belonging compensation unit works as a filter removing nearly all harmonics in the load current and voltage. The dimensioning criterion for the submodule capacitance is therefore not necessarily the load but the converter performance and the grid. The unsophisticated load may also cause a reduced switching frequency compared to converters used in other applications to be acceptable. A reduced switching frequency will cause larger voltage differences between the submodule capacitors and cause the internal currents in the converter to increase, but will at the same time reduce the switching losses.

6 Discussion

6.1 Simulations and converter performance

The simulations have verified the behavior of the model, and it is shown that it performs according to relevant theory. The simulation model is thus suited for studies on single-phase MMCs in general, but especially on DEH application, as it has a control system designed for this purpose. The control system has purposely been kept relatively simple, as no complex control is required. A simple system is also more intuitive for other users and makes it more straight forward to make modifications and adaptions, if required in the future.

In the dimensioning of the system, the main emphasis has been placed on achieving a good performance of the converter solution from a technical perspective. Investment cost has not been considered, as it is beyond the scope of the thesis. However, in [46] it is shown that the cost of the MMC will be comparable to that of a SC-HB. The low complexity of the DEH load may also allow for certain parts of the converter to be downscaled compared to converters for other kinds of load, thus reducing costs.

As the DEH load consumes a large amount of active power, it is important to achieve high overall system efficiency. The losses in the converter have not been quantified, but different possibilities to reduce them have been highlighted. These include implementation of the reduced switching frequency algorithm, selecting a filter that contributes to reduced internal currents in the converter, and the possibility to reduce the frequency of the triangular carrier frequency in the PWM-algorithm. All these factors can help reduce the losses in the converter and will also contribute to a lower cooling requirement and reduced internal temperature in the converter, which again will have a positive influence on the expected lifetime and reliability of components. Although low converter losses are important, one of the key factors favoring a power electronics solution for DEH is the possibility to operate at higher frequencies. This is believed to increase the share of current flowing through the pipeline, and this is where the largest potential in energy savings is believed to be.

MMCs are known to have circulating currents increasing losses in the converter. It is shown that in the single-phase MMC, the internal currents flow between the DC-link and the converter legs and not between the different legs as is the case for three-phase inverters. The internal currents can be limited by utilizing an appropriate filter on the DC-link. The large single-phase load will draw a varying instantaneous current, and this filter is introduced to keep the harmonics on the grid sufficiently low. A filter is likely to be required independent of the chosen converter topology, due to the mention single-phase load. The internal current of the MMC is one of its drawbacks, but can for single-phase operation be greatly reduced by a component that must be present either way. This emphasizes the suitability of the MMC in single-phase applications such as DEH.

The dynamic performance and fault handling capabilities of the converter have not been a focus in this thesis, and no protection schemes are discussed. During normal operation, the converter only need to supply a constant voltage and frequency, thus it has seemed more relevant to achieve acceptable performance under these conditions. The protection of the converter and the load are topics recommended for further work. The current controller implemented takes care of converter starting and stopping, and it can adjust power depending on the heating requirement. It will also be able to protect the converter in case of a short circuit in the far end of the piggyback cable, but is not primarily intended for protection purposes.

6.2 The MMC as alternative to the existing solution

The MMC appears to be a good alternative to the solution used today, which is based on passive elements, as illustrated in Figure 3. The key argument for the use of a power electronic converter is the ability to increase frequency and achieve higher efficiency. To fully reveal the potential of efficiency increase, a system operating at higher frequency must be installed. The risk of this should not be too large, as converters are extensively used for other purposes, and it is unlikely that such a solution should give any reduced performance compared to existing solutions even if the efficiency turns out not to increase.

Further, the complex tuning of the balancing circuit required by the existing solution would be avoided if a power electronics converter is used. The converter solution does also require tuning of a filter, but this can be achieved significantly simpler by adjusting the output frequency. The converter can also effortlessly adjust the output power to any value required by the operating mode of the pipeline. This is a contrast to the existing solution, requiring a transformer with tapping to control the output power.

Protection has not been discussed in this thesis, but it seems safe to reasons that a power electronic converter will offer a very good short circuit protection of the load, as the IGBTs can break the short circuit current within very short time. This is an improvement from the traditional solution, which has a high short circuit level at the terminals and may potentially burn hole in the pipeline in the event of a short circuit in the near end of the pipeline [10].

As discussed, one of the advantages of the MMC is its superior modularity. As DEH gains popularity and becomes established as a good alternative also outside of Norway, the need for a modular and standardized solution that can be adjusted to fit nearly any pipeline increases, and this will favor a converter solution in general, and the MMC in particular.

Conclusion

Current DEH systems operate at grid frequency and suffer from poor efficiency, as a large share of the load current flows in the sea water parallel to the pipeline. It is believed that operation at an increased frequency can reduce the sea water current and give increased system efficiency. To achieve this, a power electronic converter must be utilized. The Modular Multilevel Converter has been shown to be the most promising due to its superior flexibility and modularity, as well as its wide operating range. These are attributes that makes it possible to develop a solution made from standardized components that can be adapted to fit a wide range of pipeline systems.

A simulation model of the MMC has been developed in MATLAB Simulink, and a customized control system has been implemented. Simulations have validated the performance of the model and have made it possible to dimension a system with an acceptable performance. The 2nd harmonic power oscillations influencing the grid are among the main challenges in achieving satisfactory performance. The resonant band-stop filter reduces the oscillations, and in addition has positive influence on the internal currents of the converter. It has been shown that for DEH application, it is possible to tune the filter by adjusting the output frequency within a small range, thus ensuring simplified commissioning and satisfactory operation.

It is shown that the circulating current found in three-phase MMCs is a phenomenon not seen in single-phase MMCs, as the total energy stored in the capacitors of the two legs oscillate in phase. Instead, there is a potential for current flowing between the submodules and the grid. Since these are efficiently limited by the band-stop filter, the arm inductance intended to reduce the circulating current can be downscaled, thus saving weight. A rough weight estimation of key components has been performed, and a summary is found in Table 16.

Table 16: Weight estimate of key components

Component	Weight [kg]
Input transformers	3x3100
SM capacitors	500
Comp. Capacitors	2000
Filter inductor	700
Arm inductors	2800
Total	**15300**

The MMC seems a promising alternative for DEH application, and has several promising features unrivaled by the existing DEH solution. In addition to higher frequency, it can offer better protection, modularity, power control and can be tuned more easily. This thesis provides a good foundation for the further studies that are required in order to develop a power electronic solution suitable for the given application.

Further work

This thesis aims to evaluate the possibility of operating DEH systems using a power electronics converter. It has not been the intention to create a complete report covering all topics that need attention before a system can be installed. There are therefore several areas that have not been discussed or investigated.

The thesis has verified the suitability of a power converter solution, and a rough dimensioning of a generic system has been performed. Detailed data on an actual system is required to perform a more thorough study that has relevance beyond that of a feasibility study.

The MMC is a relatively new topology; especially the single-phase MMC is scarcely described in literature, and the field of application is also new. The simulations should thus be verified by testing on a small scale pilot. One of the main challenges has turned out to be filtering of the 2nd harmonics occurring due to the single-phase load, and verification of filter functionality and sensitivity to non-ideal parameters will be important.

A topic not treated in this thesis, is fault analysis and protection of the load and converter. This requires further attention in order to be able to design a system that can handle faults in the converter or load without taking damage. The consequences of the common mode voltage and stray capacitances should be evaluated. Cable limitations must be investigated further, especially for long systems where the voltage may become a problem. Operating frequency limits of the cable and resonance phenomena should also be considered.

One of the main arguments for selecting a converter solution for DEH is the ability to increase the system efficiency by increasing operating frequency. To the author's knowledge, this efficiency increase is a common opinion among researchers but has not been definitely verified. Confirmation of this property would be vital in establishing this solution as an attractive alternative to the existing solution. This, along with a more detailed knowledge of load parameters variation with frequency, would help determine an optimal operating frequency the converter should be dimensioned for. These are phenomena that are difficult to establish analytically, and detailed knowledge can only be obtained by installation of a full-scale pilot.

Bibliography

1. Eric Dendy Sloan Jr, *Clathrate hydrates of natural gases,* 1998, Marcel Dekker Inc.
2. Statoil, *Kort om flerfaseteknologi*, [cited 2011 11-10], Available from: http://www.statoil.com/no/technologyinnovation/fielddevelopment/flowassurance/pages/aboutflowassurance.aspx
3. V Lachet, E Duret, E Heintze and V Henriot, *Control of hydrate formation in flow lines during transport or shutdowns,* 2001, Multiphase '01
4. Arne Nysveen, Harald Kulbotten, Jens Kr. Lervik, Atle H. Børnes and Martin Høyer-Hansen, *Direct Electrical Heating of Subsea Pipelines - Technology Development and Operating Experience,* 2005, IEEE Transactions on Industry Applications
5. Canadian Association of Petroleum Producers, *Prevention and Safe Handling of Hydrates*, [cited 2011 23.11], Available from: http://www.capp.ca/getdoc.aspx?DocId=67103&DT=NTV
6. Svein Tønseth, *Verdifull kur mot kalde plugger*, Xergi, 1-2010
7. John J. Carroll, *Natural Gas Hydrates - A Guide for Engineers,* 2009, Gulf Professional Publishing
8. Harald Kulbotten and Jens Kristian Lervik, *Direct Electrical Heating System for Preventing Wax and Hydrates in Pipelines,* 2007
9. Nexans, *Tyrihans - Longest in the world*, [cited 2011 14.12], Available from: http://www.nexans.com/eservice/Corporate-en/navigate_276914/Tyrihans.html
10. Asle Skjellnes and Are Johan Hansen, *DEH with power electronic converters for the Njord platform,* 2011, Siemens AS
11. Daniel Mayer and Petr Kropik, *New approach to symmetrization of three-phase network,* 2005, Electrical Engineering
12. Asle Skjellnes, Verbal communication, 2011-2012, Siemens AS
13. Harald Kulbotten, Verbal communication, Fall 2011, SINTEF
14. Jens Kristian Lervik, Harald Kulbotten, Arne Nysveen and Martin Høyer-Hansen, *Electromagnetic modelling for electrical heating of pipelines*, *HES-07 International Symposium on Heating by Electromagnetic Sources*, Padova
15. Company visit, 2011, Bredero Shaw
16. Geir Endal, *Utviklingstrekk for feltrørledninger,* 2011, Statoil
17. Lars Gåsø, Verbal communication, 2011, Bredero Shaw
18. Nexans, 2007, Model available at NTNU Gløshaugen

19. Atle Børnes, *Direct Electrical Heating (DEH) - System Design and Technology Development,* 2011, Statoil
20. Penn Energy, *Direct heating safeguards flow through harsh-environment pipelines*, [cited 2012 23.01], Available from: http://www.pennenergy.com/index/petroleum/display/309514/articles/offshore/volume-67/issue-10/transportation-amp-logistics/direct-heating-safeguards-flow-through-harsh-environment-pipelines.html
21. Sivert Eliassen, *Efficiency improvements in Direct Electrical Heating systems by increasing operating frequency,* 2011, NTNU
22. Ned Mohan, *Electric Drives - An integrative Approach,* 2003, MNPERE
23. Siemens AG, *ROBICON Perfect Harmony - the leading medium-voltage drive*, [cited 2012 03.02], Available from: http://www.automation.siemens.com/mcms/infocenter/dokumentencenter/ld/Documentsu20Brochures/mv-umrichter/ws-perfect-harmony-en.pdf
24. D. Grahame Holmes and Thomas A. Lipo, *Pulse Width Modulation for Power Converters,* 2003, John Wiley & Sons
25. Espen Haugan, Verbal communication, 2011-2012, Siemens AS
26. Justin Gerdes, *Siemens Debuts HVDC PLUS with San Francisco's Trans Bay Cable*, [cited 2012 03.02], Available from: http://www.energy.siemens.com/hq/pool/hq/energy-topics/living-energy/issue-5/LivingEnergy_05_hvdc.pdf
27. A. Lesnicar and R. Marquardt, *An innovative Modular Multilevel Converter Topology Suitable for a Wide Power Range,* 2003, IEEE Bologna PowerTechConference
28. Lars Norum, Anandarup Das and Hamed Nademi, *A method for Charging and Discharging Capacitors in Modular Multilevel Converter*, NTNU
29. *Basics of M2C topology,* 2008, Siemens AG
30. Infineon, *1700 V IGBT single switch product family*, Available from: http://www.infineon.com/cms/en/product/power-modules-and-discs/igbt-modules/igbt-modules-up-to-1600v/1700v/igbt-modules-up-to-1600v/1700v-single-switch/channel.html?channel=ff80808112ab681d0112ab69f0e40382
31. Siemens AG, *Robicon Perfect Harmony - Medium Voltage AC Drives,* 2005, Siemens Energy & Automation
32. Post Doc Anandarup Das, *Simulink model of 3-phase MMC,* 2012
33. Nexans, *Direct Electrical Heating*, 2012

34. Arne Nysveen, *Maritime and Offshore Power Systems,* 2011, NTNU
35. John J. Grainger and William D. Stevenson, *Power System Analysis,* 1994, McGraw-Hill
36. Post Doc Anandarup Das, Verbal communication, Spring 2012, NTNU
37. Jens G. Balchen, Trond Andresen and Bjarne A. Foss, *Reguleringsteknikk,* 2003, NTNU Trykk
38. Finn Haugen, *The Good Gain method for PI(D) controller tuning*, 2012
39. Quingrui Tu, Zheng Xu and Lie Xu, *Reduced Switching-Frequency Modulation and Circulating Current Suppression for Modular Multilevel Converters,* 2011, IEEE Transactions on Power Delivery
40. Ned Mohan, Tore M. Undeland and William P. Robbins, *Power Electronics - Converters, Applications and Design,* 2003, John Wiley & Sons, Inc
41. Jan Machowski, Janusz W. Bialek and James R. Bumby, *Power System Dynamics - Stability and Control,* 2008, John Wiley & Sons, Ltd
42. Pioneer Electric, *Dry Type Power Transformers*, 2011
43. Ducati Energia, *Power Electronic Capacitors*, [cited 2012 29-05], Available from: http://ducatienergiafiles.demoshots.it/prodottipdf/Power%20Electronics_ENG.pdf
44. Qingrui Tu, Zheng Xu, Hongyang Huang and Jing Zhang, *Parameter Design Principle of the Arm Inductor in Modular Multilevel Converter based HVDC*, *2010 International Conference on Power System Technology*, Hangzhou, China
45. Circutor, *CHV-M Single-phase capacitor*, Available from: http://www.circutor.com/docs/ft_r8-9_gb-chv-m.pdf
46. Marc Hiller, *A new highly modular medium voltage converter topology for industrial drive applications*, *European Conference on Power Electronics and Applications*, Barcelona
47. Hamed Nademi, Verbal communication, 2012, Phd. Student, Siemens AS
48. James W. Nilsson and Susan A. Riedel, *Electric Circuits,* 2005, Pearson - Prentice Hall
49. IEEE, *Recommended Practices and Requirements for Harmonic Control in Electrical Power Systems,* 1992
50. REO, *A Practical Guide for EN 61000-3-3 and EN 61000-3-11*, Available from: http://www.reo.co.uk/files/handbook_en_61000-3-3_and_en_61000-3-11.pdf
51. Arne Nysveen, *TET 4195 High Voltage Equipment - Power Transformers,* 2011, NTNU

Appendices

A Current controller tuning

The PI controller used in the current controller loop has been tuned using the Good Gain method. The method is experimental and can be used on both simulation models and actual systems. A thorough documentation of the Good Gain method is found in [38], while a brief description of the method and obtained results are given in the following.

A.1 Good Gain method

1. The process must first be brought close to the normal operating point by adjusting the control signal manually.
2. At this stage, set the controller to be a pure proportional controller by setting the integrator time constant, $T_{i,}$, to infinity. A step in the reference is applied, and the proportional gain, K_p, is gradually increased from 0 until one obtains satisfactory stability. Some overshoot and a small undershoot should be observed. In this process, it is important that saturation in the controller or process is avoided. The gain value obtained is noted, and denoted K_{pGG}.
3. The time between the first overshoot and the first undershoot is recorded and denoted T_{ou}. The integral time, T_i, to be used in the controller is equal to

$$T_i = 1.5T_{ou} \tag{A.1}$$

4. As the integrator term now has been introduced, the proportional gain should be decreased somewhat in order to maintain stability. The Good Gain method suggests using

$$K_p = 0.8K_{pGG} \tag{A.2}$$

5. Run the system with the values obtained in the previous steps and check the stability of the system. Check if the system has satisfactory stability, and if required, reduce Kp or increase Ti.

A.2 Controller tuning

The current controller and DEH system can be represented by the model shown in Figure 46. The load is compensated so that the converter sees a unity PF load in steady state. However, the large inductive and capacitive parameters affect the transient behavior of the system.

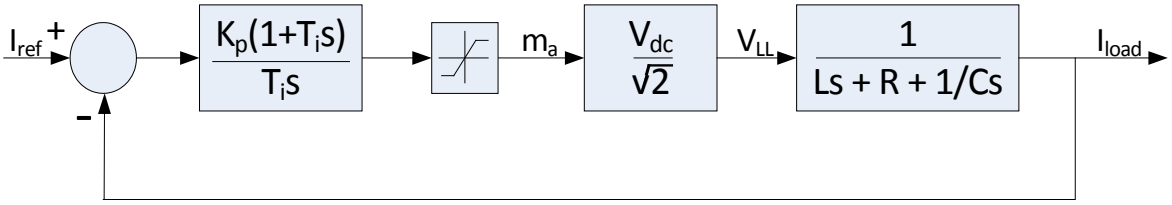

Figure 46: Detailed current controller

The PI-controller has been tuned according to the procedure described above. A pure proportional controller is applied during a step in the current reference. The response in Figure 47 is obtained by trial and error, thus satisfying the criteria in step 2 of the procedure above. A steady-state deviation from the reference is observed and is due to the integrator not being applied at this stage.

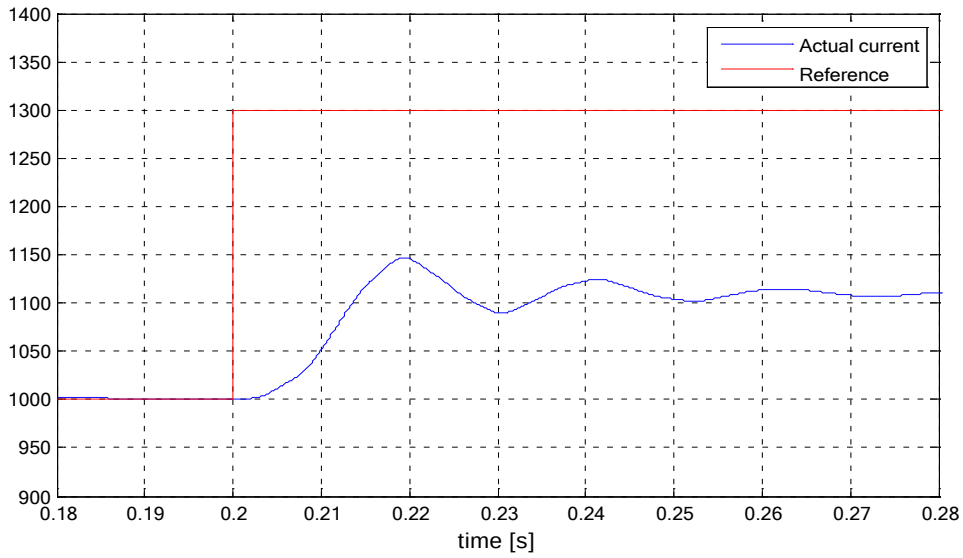

Figure 47: Current step response with proportional regulator, Kp=0.003

From the figure the following values for K_{pGG} and T_i are obtained:

$$K_{pGG} = 0.003\,,\; T_{ou} = 0.01s$$

Using equation (A.1) and (A.2) we obtain

$$K_p = 0.0024\,,\; T_i = 0.015s$$

as the suggested values to use with the controller. The current response obtained using these parameters is shown in Figure 48.

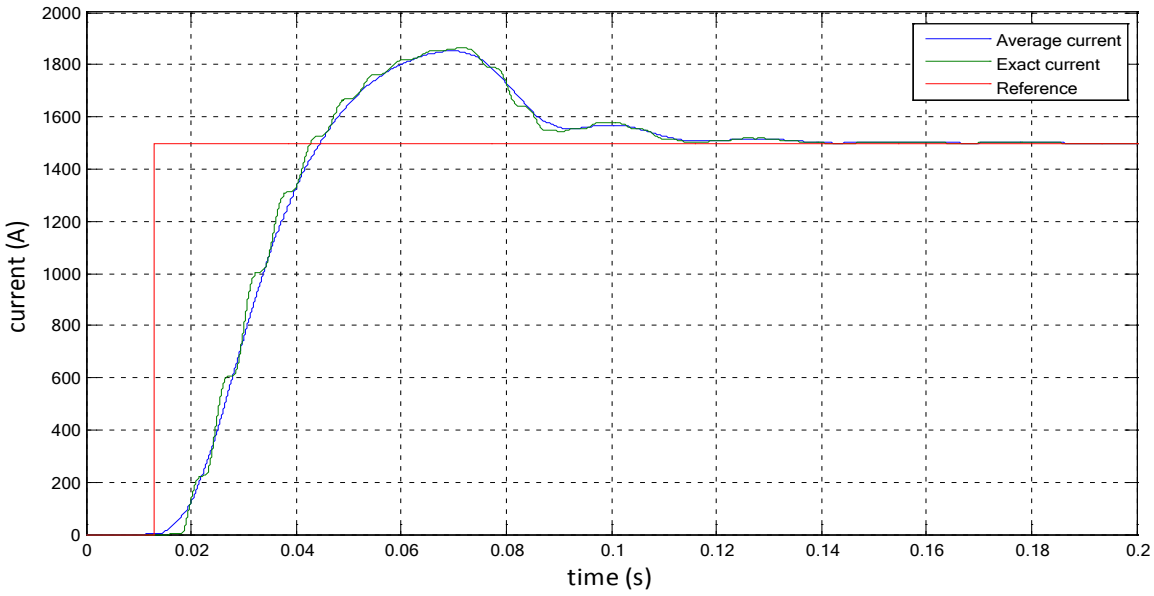

Figure 48: Current response using suggested parameters

The figure indicates that using these parameters makes the current reach the desired value within less than 0.15 s. However, the controller is too aggressively tuned, as it causes an undesired overshoot. The response time in this kind of application is of minor interest, and a slower controller can therefore be used. To find suitable parameters for the controller, the integral time constant is gradually increased until a satisfactory system behavior is reached.

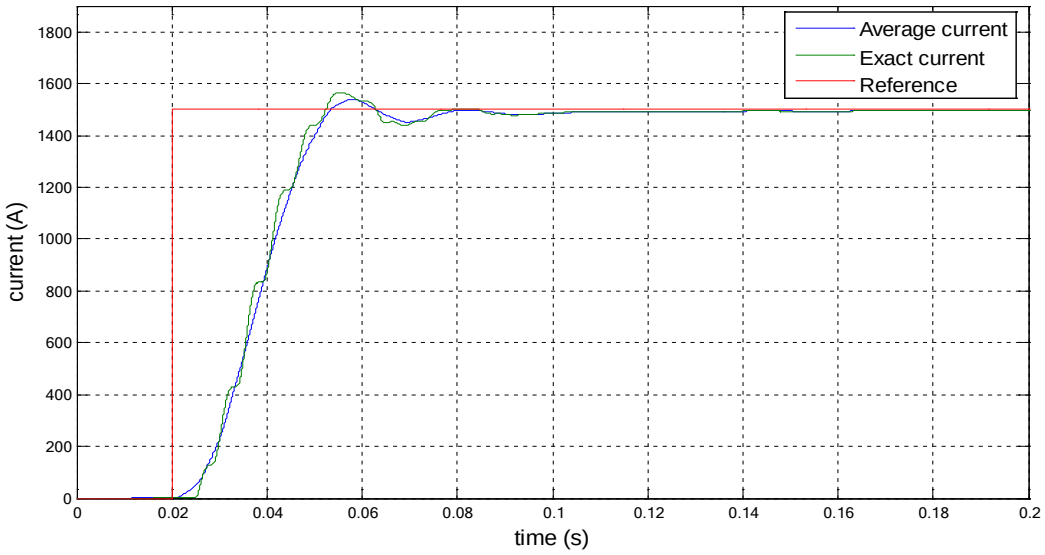

Figure 49: Current response using increased integration time

In Figure 49, a good time response is achieved where the overshoot is small, and the current reaches the desired value within short time with zero steady state error. The parameters used when obtaining Figure 49 are

$$K_p = 0.0024\ ,\ T_i = 0.06s$$

The tuning of the controller has been executed at an output frequency of 90 Hz, representing the upper range of an expected operating frequency. Using lower output frequencies will give a slower response. The model should therefore remain stable even if the output frequency is reduced. If a faster time response is desired at low frequencies, increasing the gain K_p and/or decreasing the integration time constant T_i may be considered. Using these new values at higher frequencies may however lead to an unstable system.

B Load modeling

There are several factors making it difficult to determine realistic parameters to use in the load modeling. As discussed in Section 2.1, the power factor of operating DEH systems is typically in the range of 0.25-0.3. However, these are values obtained from operation at grid frequency. To the author's knowledge, no data on how the power factor and load parameters change with frequency is known. As the load is assumed to be a series RL-circuit, the load power factor can be expressed as

$$PF = \cos\varphi = \frac{R}{\sqrt{R^2 + (\omega L)^2}} \ , \ \ \omega = 2\pi f \tag{B.1}$$

Knowing the power factor at 50 Hz, an estimation of the power factor at other frequencies can be made, assuming R and L are constant parameters. However, the resistance cannot be regarded constant in a DEH load. A thorough discussion of factors influencing the resistance is given in [21], but it can be mentioned briefly that both skin effect and proximity effect generally will increase the resistance of both cables and pipeline, due to a more uneven current distribution. The same phenomena can be observed in the water parallel to the pipe. The skin depth, δ [m], is given as:

$$\delta = \sqrt{\frac{\rho}{\pi f \mu}} = \sqrt{\frac{1}{\pi f \mu \sigma}} \tag{B.2}$$

where

- ρ = material resistivity [Ωm]
- f = frequency [Hz]
- μ = magnetic permeability of conductor [H/m]

DEH pipelines can be made from different materials having different parameters, and magnetic properties are known to vary widely even within a batch [14]. Further, it is believed that the efficiency of a DEH system will improve with operation at higher frequencies, due to a higher share of the current flowing in the pipeline instead of through the water, thus reducing the power requirement, but no reliable data confirming and quantifying this is available.

As a result, it is difficult to make an accurate model resembling the behavior of the load at different frequencies. One possible solution would be to model the load with constant resistance and inductance, and accept that this, at best, will be a rough estimate. To try reducing the error caused by uncertain load parameters and improve the accuracy of the dimensioning calculations, a data set of frequency dependent resistances in DEH pipelines found in [21] has been used. The

resistances obtained there were found by modeling a 2D DEH-load with typical dimensions in COMSOL Multiphysics, and it accounts for the aforementioned skin effect and proximity effect.

Table 17: Pipeline resistance for pipeline with μ_r=20 [21]

f [Hz]	R [Ω
50	0.0446
75	0.0581
100	0.0697

Table 17 shows the resistances obtained in the COMSOL study. These values have then been normalized using the 50 Hz value as base, since the power factor, assumed to be 0.25, is relatively certain at this frequency. Using linear regression on the normalized data set, an expression for resistance has been obtained:

$$R = (0.01125f + 0.439) \cdot R_{50} \tag{B.3}$$

Where

- R_{50} = load resistance at 50 Hz

Equation (B.3) has been implemented into the Simulink model to make the model more realistic than if assuming a constant resistance. It must be stressed, that although this is believed to improve accuracy, it is nothing more than a best guess based on limited data. It is also based on data in the range from 50 to 100 Hz, and application outside this range will decrease its accuracy. Still, a quick inspection of equation (B.2) reveals that the skin depth alone would account for an increase in resistance of 41 % when the frequency is doubled, assuming a pipeline of large diameter compared to the skin depth and thicker than the skin depth. The corresponding increase of 56 % found in Table 17 does therefore seem quite reasonable. The inductance has been assumed constant, as no data suggesting otherwise is available.

C Weight estimation of filter

The weight of the filter components and arm inductors discussed in section 5.3.5 and 5.4 have been obtained from data sheets. It was argued that the size of the inductor was comparable of a transformer with an apparent power rating given as

$$S = p \cdot \omega L \cdot \frac{\hat{I}}{\sqrt{2}} \cdot \frac{I_{rms}}{2}$$

Further, in [51] it is shown that if the all physical dimensions [m] increase with a factor k, the weight increase with k^3, and the power rating increases with k^4. From this a relationship between weight and power rating can be derived:

$$m = m_0 \cdot k^3$$

$$k = \left(\frac{S}{S_0}\right)^{1/4}$$

Combining these give

$$m = m_0 \left(\frac{S}{S_0}\right)^{3/4} \tag{C.1}$$

This relationship makes it possible to approximate the weight of the transformer from its rating and knowledge of the weight of transformers in a relatively near range. The weight of dry type transformers have been obtained from [42]. In Table 18, the weight of transformers in the relevant power range obtained from datasheets are listed along with the estimated weight of the inductors shown in Table 13. All values obtained are approximations.

Table 18: Inductor weight estimation

Rating [kVA]	Datasheet weight [kg]	Estimated weight [kg]
102		400
228		700
240		700
300	860	
380		1000
500	1270	
750	1450	
1000	1800	
1500	3100	
1620		3200

The weight of filter capacitors have been obtained from [43], using the GP84 series which are general purpose AC capacitors suitable for filters and resonant circuits. The capacitors have been selected to maintain a minimum safety margin of 20 % in terms of both capacitor current and voltage.

D MATLAB Simulink simulation model

D.1 Rectifier model

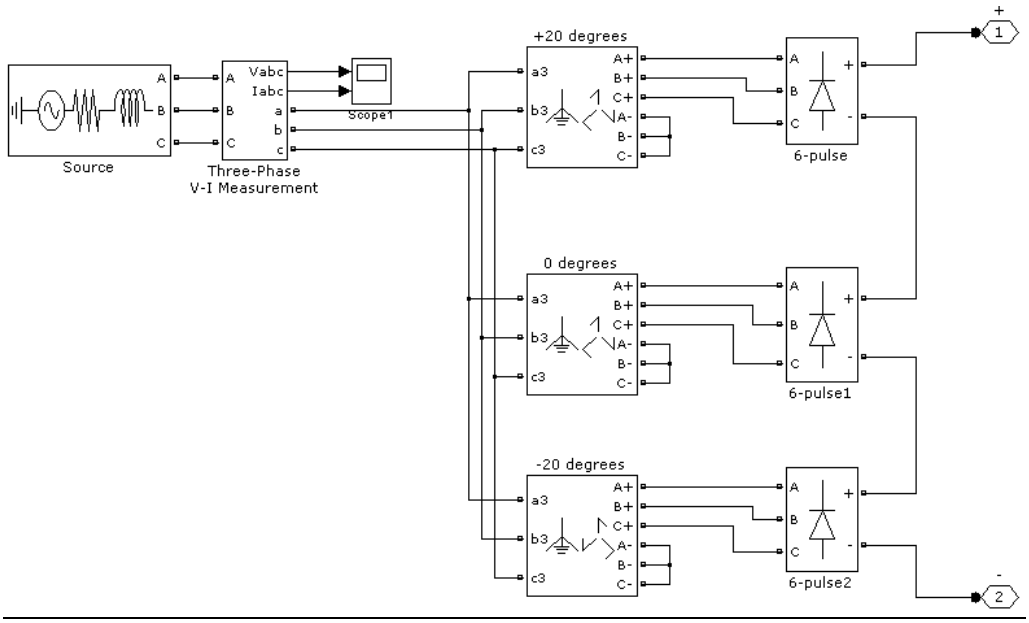

D.2 Current controller

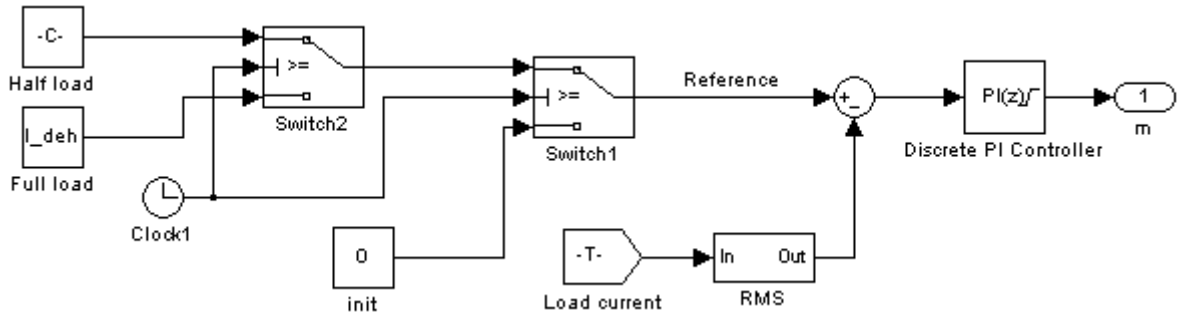

D.3 Resonant band-stop filter

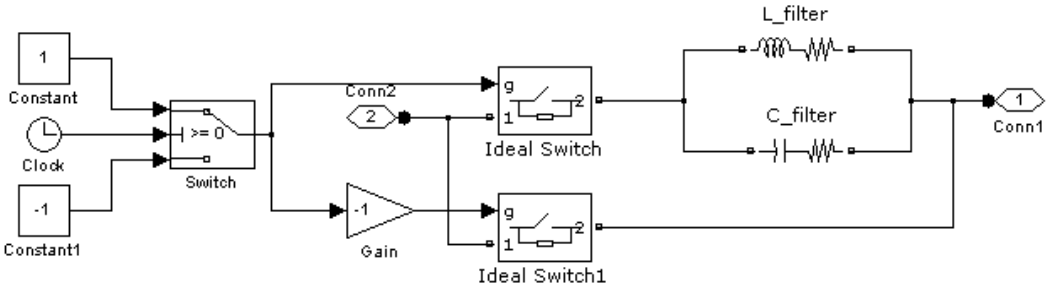

D.4 PWM-algorithm

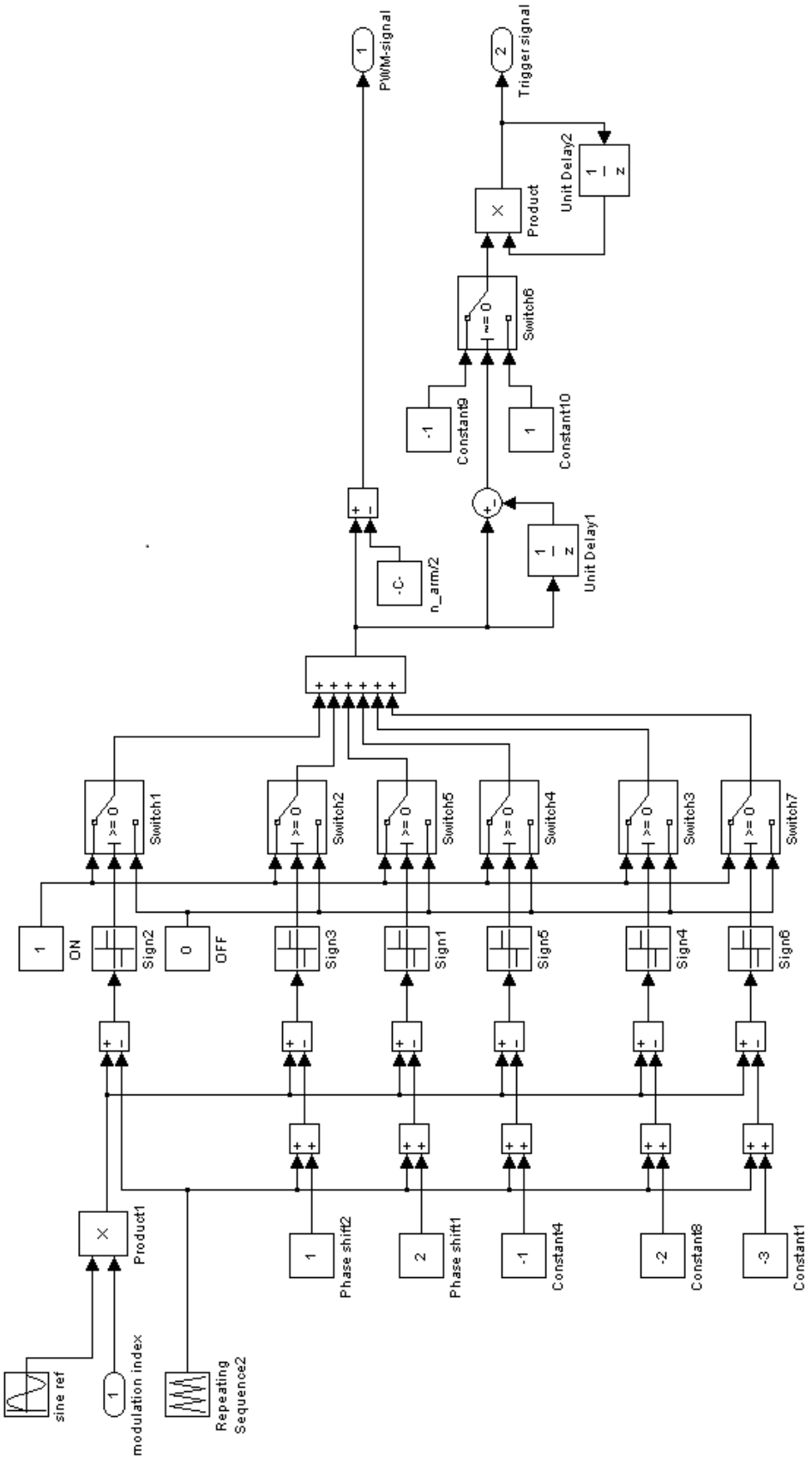

D.5 Control of leg arms

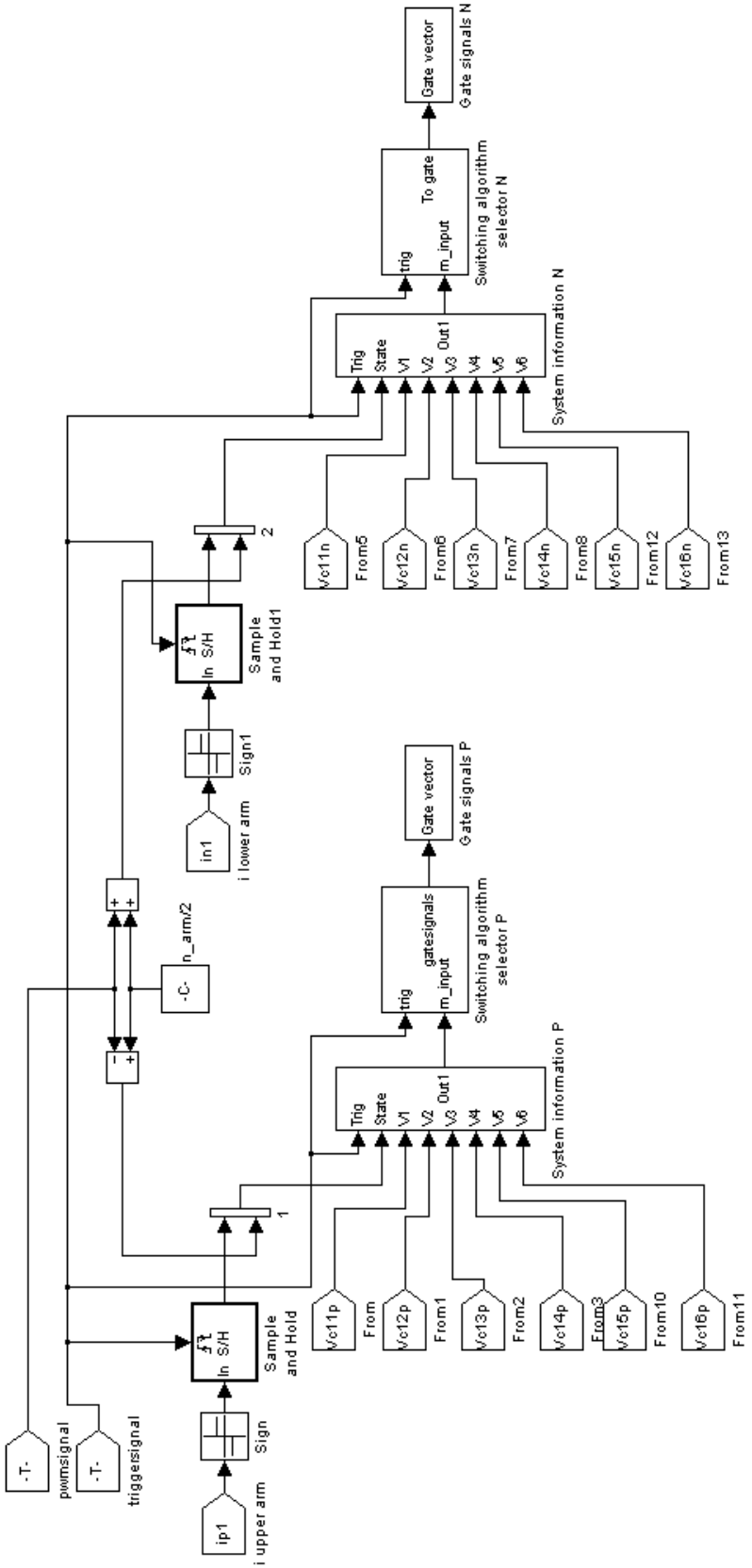

E Simulation model parameters

```
clear all
clc
sampletime=5e-6;        %Simulation sample time (s)

%%%%%%%%%%%%%%Input circuit%%%%%%%%%%%%%%%%
V_utility=11e3;         %Utility voltage (V)
f_utility=50;           %Utility frequency (Hz)
R_tr=0.01;              %Transformer resistance (pu)
L_tr=0.07;              %Transformer inductance (pu)

%%%%%%%%%%%%%%Converter data%%%%%%%%%%%%%%%%
P_max=4e6;              %Max. power delivered to load (W)
S_conv=1.1*P_max;       %Converter rated power (VA)
I_max=1500;             %Max output current (A)
n_arm=6;                %Number of submodules per leg arm
c_sub=6E-3;             %Submodule capacitor capacitance (F)
m_f=40;                 %Frequency modulation ratio
R_arm=0.01;             %Resistance in arm RL-branch (Ohm)
L_arm=0.001;            %Inductance in arm RL-branch (H)
PF_nom=1;               %Nominal converter operating power factor
Ron=0.00001;            %Submodule switch internal resistance (Ohm)

%%%%%%%%%%%%%%%%Load data%%%%%%%%%%%%%%%%%%
P_load=4e6;             %Active load power required (W)
PF_50=0.25;             %Load power factor at 50 Hz (inductive)
f_ac=75;                %Output frequency (Hz)

%%%%%%%%%%%%%%Control%%%%%%%%%%%%%%%%%%%%%%
dVc_lim=[100, 100, 100; 100, 100, 100];
                        %Limit for activation of normal switch algorithm (V)
k_pi=0.001;             %Current control proportional gain
T_ii=0.03;              %Current controller integrator time
PImax=1;                %PI-regulator upper limit (default = 1)

%%%%%%%%%%Calculated parameters%%%%%%%%%%%%
R_50=P_max/I_max^2;     %Load resistance at 50 Hz (Ohm)
R_load=(0.01125*f_ac+0.439)*R_50;
                        %Frequency dependent load resistance (Ohm)
I_deh=sqrt(P_load/(R_load));
                        %Required load current to meet power demand (A)
Vdc=((sqrt(2)*S_conv/(I_deh))/PF_nom+0.6*I_max*(sqrt((R_arm)^2+(2*pi*f_ac*L_arm)^2)
));                      %Required DC-link voltage (V)
L_load=R_50/(100*pi)*tan(acos(PF_50));
                        %Load impedance[H]
C_load=1/(2*pi*f_ac)/(2*pi*f_ac*L_load-sqrt(R_load^2/PF_nom^2-R_load^2));
                        %Series compensating capacitor capacitance (F)
vc_sub_init=Vdc/n_arm;  %Submodule capacitor initial voltage (V)
f_pwm=f_ac*m_f;         %Frequency of pwm-signal (Hz)
T_pwm=1/f_pwm;          %Carrier signal period (s)
Cs=0.5*P_load/(1000*2*pi*50*(Vdc/(1.35*2)^2));
                        %IGBT snubber capacitance (set to ensure
                        %numerical stability)(F)
Rs=4*sampletime/Cs;     %IGBT snubber resistance (set to ensure
                        %numerical stability)(Ohm)
k_ii=k_pi/T_ii;         %Current control integrator gain
C_filter=1e-3;          %Band-stop filter capacitance (F)
L_filter=1/(C_filter*(4*pi*f_ac)^2);
                        %Band-stop filter inductance (H)
R_filter=20e-3;         %Band-stop filter resistance (Ohm)
```

F Switching algorithm MATLAB code

F.1 Normal switching algorithm

```
function [gatesignal] = moduleselector_normal(voltvector)
%function y = fcn(voltvector)
%#codegen

%-------------------------------------------------------
%The first block of code determines how many
%modules should be ON and OFF in the next interval
%-------------------------------------------------------
armcount=(max(size(voltvector))-1);
modulesOFF=voltvector(1,2);
gatesignal=ones(armcount+1,1);

%-------------------------------------------------------
%Either turns all modules OFF or ON, or creates a
%vector with all capacitor voltages and corresponding
%index number, which is then sorted in ascending order
%based on voltages.
%-------------------------------------------------------
if modulesOFF==armcount
    for i=1:armcount
        gatesignal(i)=-1;
    end
    switched=1;
elseif modulesOFF==0
    switched=1;
else
    voltages=zeros(armcount,2);
    for i=1:armcount
        voltages(i,1)=voltvector(i+1);
        voltages(i,2)=i;
    end
    [~,index]=sort(voltages, 1, 'ascend');
    switched=0;
end

%-------------------------------------------------------
%Switches either the most charged or least charged
%module depending on switching ON or OFF and the
%direction of current.
%-------------------------------------------------------
if switched==1
elseif (voltvector(1,1)==1)
    for i=(armcount-modulesOFF+1):(armcount)
        gatesignal(voltages(index(i,1), 2))= -1;
    end
elseif (voltvector(1,1)==-1)
    for i=1:(modulesOFF)
        gatesignal(voltages(index(i,1), 2))= -1;
    end
end

end
```

F.2 Reduced switching frequency algorithm

```
function [gatesignal] = moduleselector_RSF(voltvector)
%function y = fcn(voltvector)
%#codegen

%-------------------------------------------------------
%The first block of code determines how many
%modules should be ON and OFF in the next interval
%-------------------------------------------------------
armcount=(max(size(voltvector))-1);
modulesOFF=voltvector(1,2);
gatesignal=zeros(armcount+1,1);
old_OFF=0;

%-------------------------------------------------------
%Determines the number of modules ON and OFF in the
%previous sample
%-------------------------------------------------------
for i=1:armcount;
    gatesignal(i)=voltvector(i+1,2);
    if voltvector(i+1,2) <= 0
        old_OFF=old_OFF+1;
    end
end

%-------------------------------------------------------
%Initializing "voltages" unless all modules are going
%to be ON or all modules are going to be OFF
%-------------------------------------------------------
if (modulesOFF ~= old_OFF && modulesOFF ~= 0 && modulesOFF ~= armcount)
    voltages=zeros(abs(modulesOFF-old_OFF),2);
end

%-------------------------------------------------------
%If either all modules should be switched ON or all
%modules should be switched OFF, this is done directly,
%and no sorting is required. Else, the voltage and
%corresponding index number of the modules that may be
%switched are collected in an Nx2 vector.
%-------------------------------------------------------
counter=0;
if modulesOFF == 0;
    for i=1:armcount;
        gatesignal(i)=1;
    end
    gatesignal(armcount+1)=old_OFF;
    Switched=1;
elseif modulesOFF == armcount
    for i=1:armcount
        gatesignal(i)=-1;
    end
    gatesignal(armcount+1)=armcount-old_OFF;
    Switched=1;
elseif modulesOFF == old_OFF
    for i=1:armcount;
        gatesignal(i)=voltvector(i+1,2);
    end
    gatesignal(armcount+1)=0;
    Switched=1;
```

```
elseif modulesOFF > old_OFF
    voltages=zeros(armcount-old_OFF,2);
    for i=1:armcount;
        if voltvector(i+1,2) > 0
            counter=counter+1;
            voltages(counter,1)=voltvector(i+1,1);
            voltages(counter,2)=i;
        end
    end
    gatesignal(armcount+1)=modulesOFF-old_OFF;
    Switched=0;
elseif modulesOFF < old_OFF
    voltages=zeros((old_OFF),2);
    for i=1:armcount;
        if voltvector(i+1,2) <= 0
            counter=counter+1;
            voltages(counter,1)=voltvector(i+1,1);
            voltages(counter,2)=i;
        end
    end
    gatesignal(armcount+1)=old_OFF-modulesOFF;
    Switched=0;
end

%-------------------------------------------------------
%Sorts the modules that can be switched in ascending
%order based on the voltage. Switches either the
%most charged or least charged module depending on
%switching ON or OFF and the direction of current.
%-------------------------------------------------------
if Switched == 0
    [~,index]=sort(voltages, 1, 'ascend');
    if modulesOFF > old_OFF
        if voltvector(1,1)==1
            gatesignal(voltages(index(counter,1),2))= -1;
        elseif voltvector(1,1)== -1
            gatesignal(voltages(index(1,1),2))= -1;
        end
    elseif modulesOFF < old_OFF
        if voltvector(1,1) == 1
            gatesignal(voltages(index(1,1),2))= 1;
        elseif voltvector(1,1) == -1
            gatesignal(voltages(index(counter,1),2))= 1;
        end
    end
end

end
```